Dual Control of Depositional Facies on Uranium Mineralization in Coal-bearing Series: Examples from the Tuanyushan Area of the Northern Qaidam Basin, NW China

GUO Biao[1, 2], SHAO Longyi[1, *], WEN Huaijun[3], HUANG Guangnan[3], ZOU Mingjun[2] and LI Yonghong[3]

1 *College of Geosciences and Survey Engineering, China University of Mining and Technology, Beijing 100083, China*

2 *School of Resources and Environment, North China University of Water Resources and Electric Power, Zhengzhou 450046, China*

3 *Qinghai Bureau of Coal Geological Exploration, Xining 810007, China*

Abstract: The uranium deposits in the Tuanyushan area of northern Qaidam Basin commonly occur in coal-bearing series. To decipher the U-enrichment mechanism and controlling factors in this area, a database of 72 drill cores, including 56 well-logs and 3 sampling wells, was examined for sedimentology and geochemistry in relation to uranium concentrations. The results show that coal-bearing series can influence uranium mineralization from two aspects, i.e., spatial distribution and dynamic control. Five types of uranium-bearing rocks are recognized, mainly occurring in the braided river and braided delta sedimentary facies, among which sandstones near the coals are the most important. The lithological associations of sandstone-type uranium deposits can be classified into three subtypes, termed as U-coal type, coal-U-coal type, and coal-U type, respectively. The coal and fine siliciclastic rocks in the coal-bearing series confined the U-rich fluid flow and uranium accumulation in the sandstone near them. Thus, the coal-bearing series can provide good accommodations for uranium mineralization. Coals and organic matters in the coal-bearing series may have served as reducing agents and absorbing barriers. Methane is deemed to be the main acidolysis hydrocarbon in the U-bearing beds, which shows a positive correlation with U-content in the sandstones in the coal-bearing series. Additionally, the $\delta^{13}C$ in the carbonate cements of the U-bearing sandstones indicates that the organic matters, associated with the coal around the sandstones, were involved in the carbonation, one important component of alteration in the Tuanyushan area. Recognition of the dual control of coal-bearing series on the uranium mineralization is significant for the development of coal circular economy, environmental protection during coal utilization and the security of national rare metal resources.

Key words: coal-bearing series, dual control, uranium deposits, northern Qaidam Basin, Tuanyushan

1 Introduction

Sandstone-type uranium deposits are economically important in many parts of the world (Dahlkamp, 1993; Shatalov et al., 2006; Wu et al., 2009; OECD, 2014). This type of uranium deposits has been successively discovered in the Yili, Turpan-Hami, northern Qaidam, Bayingebi, Ordos, Erlian, Songliao and Yanji basins of northern China (Huang Jingbai and Huang Shijie, 2005; Zhang Jindai et al., 2008, 2012; Tong Hangshou, 2014), which accounts for approximately 80% of the uranium resources in China (Cai Yuqi et al., 2015).

Sedimentology is an important component in the study of sandstone-type uranium deposits (Galloway and Hobday, 1983; Maithani et al., 1995). In recent years, with the development of new theories and technologies, sedimentology has become increasingly important for exploration and resource evaluation of sandstone-type uranium deposits in China (Jiao et al., 2005; Yang

* Corresponding author. E-mail: shaol@cumtb.edu.cn

Renchao et al., 2007; Wu et al., 2009; Liu et al., 2017). Isochronous stratigraphic frameworks established with high resolution sequence stratigraphy were applied to identify uranium mineralized strata (Yang Minghui and Liu Chiyang, 2006; Li Shengxiang et al., 2006; Yang Renchao et al., 2007). It has been shown that sedimentary facies analysis may be used to interpret diagenesis and to predict spatial distribution of uranium-bearing sandstones (Jiao et al., 2005; Fan et al., 2007; Akhtar and Yang, 2014). The internal architectures of uranium-bearing sandstones were also examined through the analysis of internal architecture units (Jiao et al., 2005). All of these studies have built a firm foundation for uranium metallogenic prognosis in sandstone (Li Shengxiang et al., 2006; Cai Yuqi et al., 2014; Qiu Yubo et al., 2015; Chen Fenxiong et al., 2016).

Although sandstone-type uranium deposits are commonly found in coal-bearing series (Huang Jingbai and Huang Shijie, 2005; Zhang Jindai et al., 2008, 2012; Tong Hangshou, 2014; Cai Yuqi et al., 2015; Nxumalo et al., 2017), the mechanisms of the potential influence of the coal-bearing series on uranium mineralization have not been well understood. It has been known that, under specific geological conditions, coal can enrich some metals and even form metal deposits (Finkelman and Brown, 1991; Kislyakov and Shchetochkin, 2000; Seredin and Finkelman, 2008; Hu et al., 2009; Seredin et al., 2012, 2013; Jaireth et al., 2014; Dai et al., 2015). However, the mechanisms of metallic enrichment depend on the chemical properties. For uranium enrichment, it has been proposed that the genetic or spatial relationships between the uranium and coals /organic matters in the coal-bearing series could help in uranium enrichment (Wu et al., 2009; Feng et al., 2017). The abundance and mode of occurrence of uranium in coal-bearing series, especially in coal, may contain information on the original peat-accumulation environments as well as on diagenetic and epigenetic processes (Bostrom et al., 1973; Bostrom, 1983; Wignall, 1994; Gayer et al., 1999; Ketris and Yudovich, 2009; Dai et al., 2015). Additionally, the distribution of the depositional facies in the coal-bearing series can affect uranium mineralization (Jiao et al., 2005; Chen Daisheng et al., 2006; Qiu Yubo et al., 2015; Chen Fenxiong et al., 2016; Wang Feifei et al., 2017). The sandstones occurring in different sedimentary environments always contain different concentrations of uranium (Galloway and Hobday, 1983; Maithani et al., 1995; Jiao et al., 2005, 2016; Wu et al., 2009; Hou et al., 2017; Hall et al., 2017).

In China, the sandstone-type uranium deposits commonly occur in coal-bearing basins, and these deposits are adjacent to the coal seams or the fine siliciclastic sediments rich in organic matters, such as the 511 deposits in the Yili Basin, the Dongsheng deposit in the Ordos Basin, and the Qianjiadian deposit in the Songliao Basin, where in stratigraphic texture, the U-rich deposits commonly sit above the coals, are bounded by the coals, or even occur in the coals. Since the sandstone-type uranium deposits were discovered in the Lenghu area, located in the northwest of the northern Qaidam Basin, this area has received a huge attention, and subsequently, a large number of explorational wells were drilled in the other areas of the northern Qaidam coal basin, e.g., Yuqia, Tuanyushan and Hangya areas. The reservoir quality, modes of occurrence, and geologic origin of uranium in the sandstone were studied to anticipate the favorable sedimentary environments for uranium concentration. Much of this research is focused on the sandstones and the genetic environments and reservoir quality such as the sandstone thickness, porosity, and lateral or vertical connectivity have been investigated (Chen Daisheng et al., 2006; Zhang Jindai et al., 2012; Tong Hangshou, 2014; Wang Dan et al., 2015; Feng et al., 2017). However, in this study area, uranium deposits always occur in coal-bearing series, and sit directly on the coal seams or are bounded by the coal seams (Zhang Jindai et al., 2008, 2012; Wang Dan, 2015). Even though, there is a close relationship between the coal/organic matters and the uranium deposits (Wang Dan et al., 2015), and the uranium deposits are more likely to occur in braided river facies than in meandering river facies, which are more suitable for coal (or organic matters) formation (Li et al., 2014; Shao Longyi et al., 2014). Therefore, it is necessary to expound the inner connection between uranium, sandstone and coal or organic matters, and to discuss the influence of depositional facies on uranium mineralization in coal-bearing series. In this study, a database of 72 cores, including 56 well-logs and 3 sampling wells, was analyzed on sedimentology, geochemistry, and uranium concentration. The intent was to evaluate the effect of depositional facies on uranium mineralization, and modes of occurrence of uranium concentrations in coal-bearing series.

2 Geological Setting

The northern Qaidam Basin, approximately 34,000 km^2, is located at 92°15′–98°30′ E and 36°00′–39°00′ N. It is surrounded by the Altun Mountains in the northwest, the Saishiteng Mountains and Qilian Mountains in the north, and the Maoniu Mountains in the east. Geographically, this area includes Lenghu, Qianxi, Nanbaxian, Tuanyushan, Yuqia, Hongshan, Delingha and Wanggaxiu. The Qaidam Basin is a large Mesozoic–Cenozoic continental basin (Lü Baofeng et al., 2011). According to the basement nature, stratigraphic distribution, tectonic deformation, and segmentation of the fractures and uplifts, it is divided into four first-level tectonic units and 21 secondary-level tectonic units (Dai Junsheng et al., 2003). The northern Qaidam Basin is one of the secondary-level tectonic units in the Qaidam Basin (Dai Junsheng et al., 2003) (Fig. 1). It is separated from the adjacent tectonic units by large fractures that generally distribute along a northwest–southeast direction (Tang Liangjie et al., 2000; Zeng Lianbo et al., 2001). The sediment-source region mainly consists of Lower Paleozoic chlorite quartz schist, chlorite schist and griotte, Hercynian granite, and Permo–Carboniferous carbonate rocks interbedded with calcareous shale and silt mudstones (Li et al., 2014). These units form the basement of the northern Qaidam Basin, which is infilled by Mesozoic conglomerates, sandstones and mudstones, and also by Cenozoic siliciclastic sediments (Li et al., 2014). The coal-bearing formations are part of the Middle–Lower Jurassic, which consist of the Huxishan Formation (J_1h), Xiaomeigou Formation (J_1x), Dameigou Formation (J_2d), and Shimengou Formation (J_2s). They are mainly made up of conglomerates, coarse sandstones, medium- to fine-grained sandstones, siltstones, mudstones, lignites, and oil shales (Fig. 2). These units are charcoal grey in color, and are commonly known as “Black Jurassic” (Yang Yongtai et al., 2000, 2001; Jin Zhenkui et al., 2006; Yang Renchao et al., 2007; Li et al., 2014; Shao Longyi et al., 2014). The thicknesses of the Middle-Lower Jurassic and Shimengou Formation range from 123 to 1,600 m and from 51 to 653 m, respectively.

Abundant mineral resources have been explored and exploited in the northern Qaidam Basin, such as the oil and gas resources in Lenghu, Nanbaxian, and Yuqian areas, and the coal resources in Wanggaxiu, Yuqia, Dayangtou, Xidatan, Dameigou, Hangya, and Huaitoutala exploration or mining areas. Yet, very few studies focusing on the uranium resources are available since uranium exploration has made great progress in the northern Qaidam Basin only in recent years. A number of uranium deposits were discovered in Lenghu, Yuqia, Tuanyushan, and Hangya areas, where there are also rich oil, gas and coal resources (Tang Liangjie et al., 2000; Zeng Lianbo et al., 2001; Luo Xiaorong et al., 2013; Zhai Zhiwei et al., 2013).

The uranium deposits are mainly hosted by medium- to coarse-grained sandstones in the Shimengou Formation, which is adjacent to the coal (e.g., M7 and M4), with the sandstone consisting of quartz (40% to 65%), feldspar (6% to 18%), rock fragments (1% to 3%) and carbonaceous

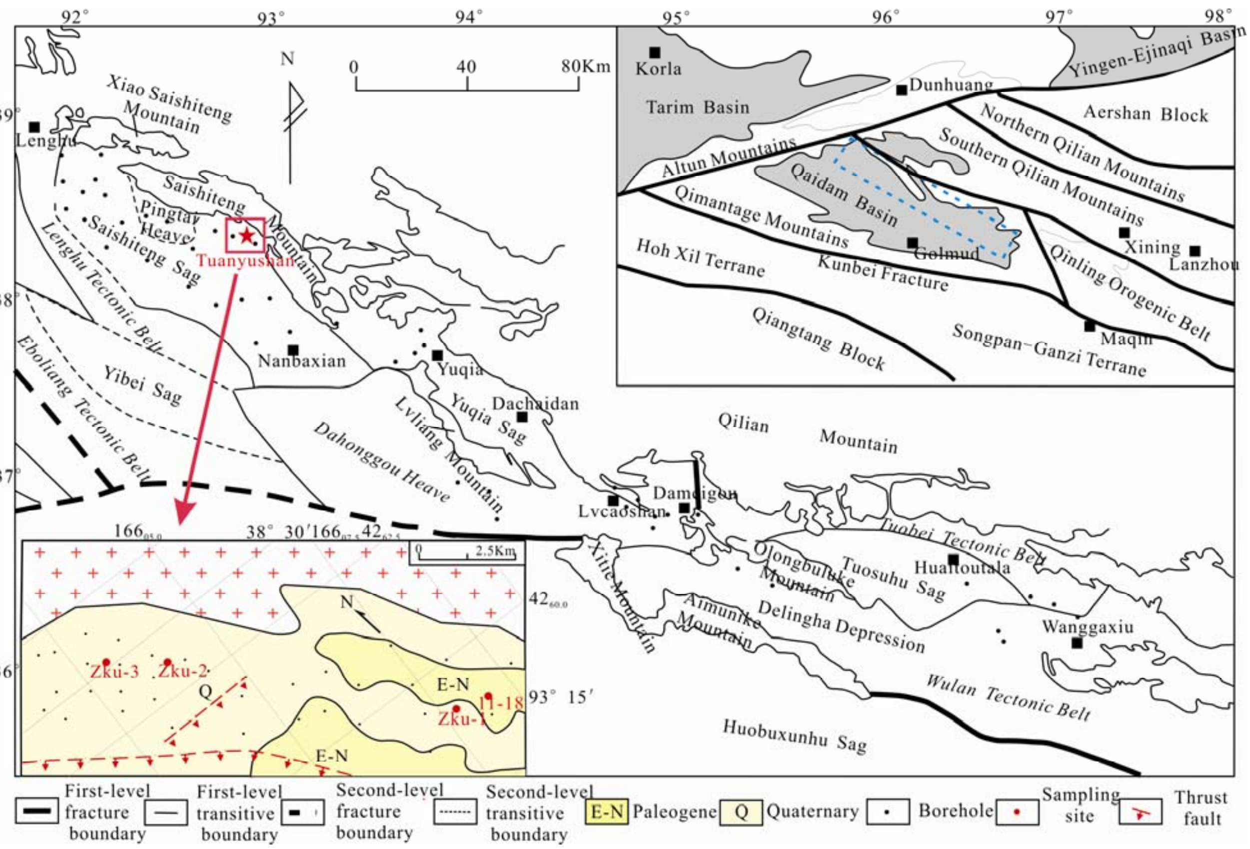

Fig. 1. Geotectonic division and location of the northern Qaidam Basin (after Dai Junsheng et al., 2003; Lü Baofeng et al., 2011), and the geological map of the Tuanyushan area in the bottom left corner.

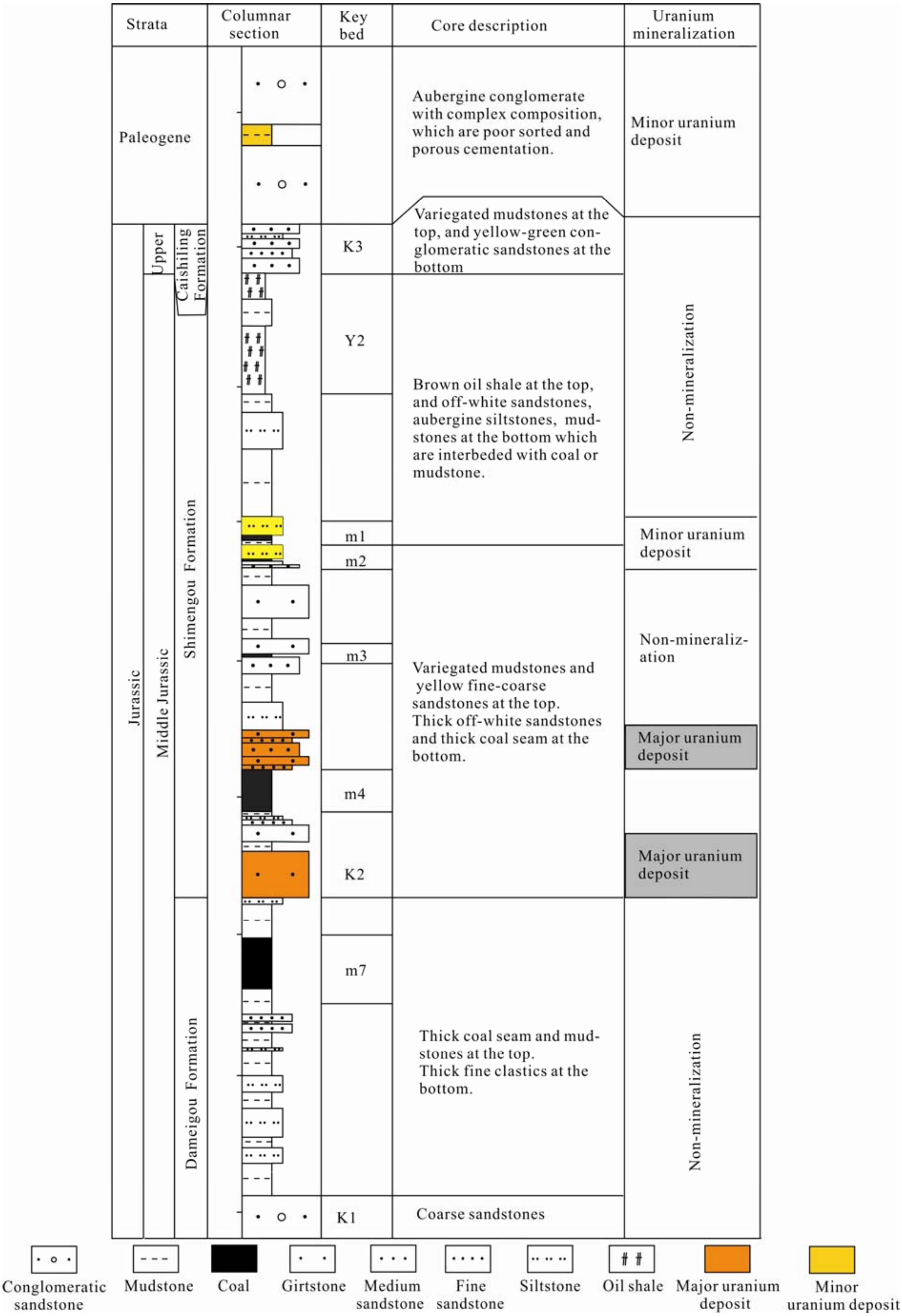

Fig. 2. Stratigraphic division of the Jurassic of borehole ZK-1 in the northern Qaidam Basin.

debris (25% to 45%).

3 Methods

Data from a total of 72 wells were collected from the study area, including 56 well-logs and five sampling cores (Zku-1, Zku-2, Zku-3, Zk8-23, and Zk11-18). These wells cover the majority of the study area.

The samples were crushed and ground to pass 200 mesh for major and trace element analysis. X-ray fluorescence spectrometry (XRF, ARL ADVANTXP+) was used to determine the oxides of the major elements, including SiO_2, Al_2O_3, Fe_2O_3, and CaO. The samples for XRF analysis were prepared by borate fusion in an automated fusion furnace (CLAISSE THEBee-10). Each sample (1 g) was mixed and homogenized with lithium borate flux (10 g; CLAISSE, pure, 50% $Li_2B_4O_7$+50% $LiBO_2$). Inductively coupled plasma mass spectrometry (ICP-MS, X-series Ⅱ), in a pulse counting mode (three points per peak), was used to determine most trace of the elements in the samples. For ICP-MS analysis, samples were digested using an UltraClave Microwave High Pressure Reactor (Milestone). The basic load for the digestion tank was composed of 330 ml distilled H_2O, 30 ml 30% H_2O_2, and 2 ml 98% H_2SO_4. The initial nitrogen pressure was set at 50 bars, and the highest temperature was set at 240°C for a period of 75 min. The reagents used for the digestion process of 50 mg sample were 5 ml 40% HF, 2 ml 65% HNO_3, and 1 ml 30% H_2O_2. Multi-element standards (Inorganic Ventures, CCS-1, CCS-4, CCS-5, and CCS-6) were used for the calibration of trace element concentrations.

The organic geochemistry analyses were conducted by the Evaluation of Oil and Gas Station, Northwest University, China. The samples were oven-dried overnight at 110°C, and were pulverized with the aid of a pestle and mortar. The crushed rock samples were analyzed geochemically for total organic carbon (TOC) content and rock-eval pyrolysis techniques in order to determine the total organic carbon and organic matter type, respectively. The acidolysis hydrocarbon testing and gas chromatographic analyses were used to determine the main types of hydrocarbons in the U-bearing sandstones. These sandstones were air-dried and crushed to pass 40 mesh. Then, under a vacuum and at 40°C, 20 g samples were taken and resolved by dilution in HCL (concentration is 1:6). The released gases, formed in the acidolysis, were filtered by alkali solution to get rid of the carbon dioxide. The remaining gases were then analyzed on a SHIMADZU Gas Chromatograph GC-14B to identify the types of acidolysis hydrocarbon. The characteristics of the flame ionization detector (FID) that were used are as follows: the chromatographic column was a fused silica capillary column (60 m in length and 0.25 mm in diameter) with OV-101 stationary liquid and a FID detector; the processor was a CR-7Ae; the injection and detector temperatures were set at 150° C; the oven temperature was set at 35°C; the carrier gases and flow rates were N_2 30 ml/min (split ratio 100/L, linear velocity 20 cm/s), clean air N_2 500 ml/min, burning gas H_2 50 ml/min, and oxidant gas Air 400 ml/min.

The C-O isotopes analysis, conducted by the Chinese Academy of Sciences Key Laboratory of Crust-Mantle Materials and Environments, was used to determine the C-O isotope composition and the material source of carbonate cement in the U-bearing sandstone. For carbon and oxygen isotope analysis, powdered carbonate samples were reacted with 100% H_3PO_4 under vacuum at 90°C for 90 minutes. Acid liberated CO_2 was then purified and the C- and O- isotopic composition was measured using a Finnigan 252 isotope ratio mass spectrometer coupled with a Finnigan Carboflo.

4 Results

4.1 Petrology and facies description

Through the analysis of the cores from the uranium-bearing formation, five types of uranium-bearing rocks, such as conglomerate, sandstone, siltstone, mudstone, and coal, were identified in the northern Qaidam Basin. According to the characteristics of the colors, textures, sedimentary structures, and plant fossils, they could be described in detail as follows.

4.1.1 Conglomerate

The U-bearing conglomerates are mainly developed at the bottom of the Shimengou Formation, and are mainly distributed along the northeastern margin of the Delingha Depression where they form a discontinuous belt of coarse conglomerates adjacent to the Oulongbuluke Mountains. The lithofacies association is made up of erosinal-based, poorly- sorted, massive conglomerates, and conglomeratic sandstones (up to 15 m in thickness) with interbedded cross-stratified sandstones. Plant fragments, stems, and leaf fossils are commonly found within them (Fig. 3). The clasts are up to 0.5–3 cm in diameter, and they consist of quartz sandstone, limestone, and granite pebbles. The predominant motif shows upward-fining cycles and imbricate arrangements in the basal conglomerates, which sit directly on the coal seams or fine siliciclastic sediments. The abnormal response features of these conglomerates on the gamma ray log are relatively low, ranging from 133 to 770 API (GRmax=7 PA/kg).

Fig. 3. Photographs of cores from the Shimengou Formation.
(a), Conglomeratic sandstone, Type 1 U-bearing sandstone; (b), Cross bedding, medium to coarse sandstone, Type 2 U-bearing sandstone; (c), Small wedge cross-bedding, fine to medium sandstone, Type 2 U-bearing sandstone; (d), Small trough cross-bedding, fine to medium sandstone, Type 3 U-bearing sandstone; (e), Convolute bedding, fine sandstone, Type 3 U-bearing sandstone; (f), Oxidized pelitic siltstone; (g), White, coarse sandstone with charcoal, Type 2 U-bearing sandstone; (h), Ripple bedding, fine sandstone, Type 3 U-bearing sandstone; (i), Oil shale; (j), Lamellibranch; (k), Leaf fossil; (l), Roots and stem fossils.

4.1.2 Sandstone

The U-bearing sandstones are widely spread out in the northern Qaidam Basin and are deemed to be a major source of U for industrial utilization (Zhang Jindai et al., 2008, 2012). Based on the rock textures, sedimentary structures and lithofacies associations, three types of U-bearing sandstones can be recognized in the Middle Jurassic in this area.

(1) Type 1 U-bearing sandstone

This type of U-bearing sandstone mainly represents the sandstone that sits directly on top of coal (U-coal type), and it occurs in the lithofacies association (up to 5–23 m in thickness), consisting of scour-based, poorly- sorted, directional conglomerate, cross-bedding sandstone, and thin siltstone or mudstone (Figs. 3a and 4). The basal fine conglomerates or conglomeratic sandstones, which range from 0.5 to 4 m in thickness, overlie the scoured surfaces, and display an imbricate arrangement. The overlying sandstones (mainly debris-feldspar-sandstones), are characterized poorly-sorted and low textural maturity by medium- to coarse-grained and trough cross-bedding ranging from 2 to 8 m in thickness. The top lithology consists of thin, horizontal-bedding siltstones or mudstones. Plant fragments, stems, and leaf fossils are commonly found within them. In addition, the hydromicazation, chloritization, and carbonatization can be found in this type of sandstone (Figs. 5a and 5b). Specifically, carbonatization existed throughout most of the uranium mineralization process (Fig. 5c). Calcite is an important cementing material in the U-bearing sandstone.

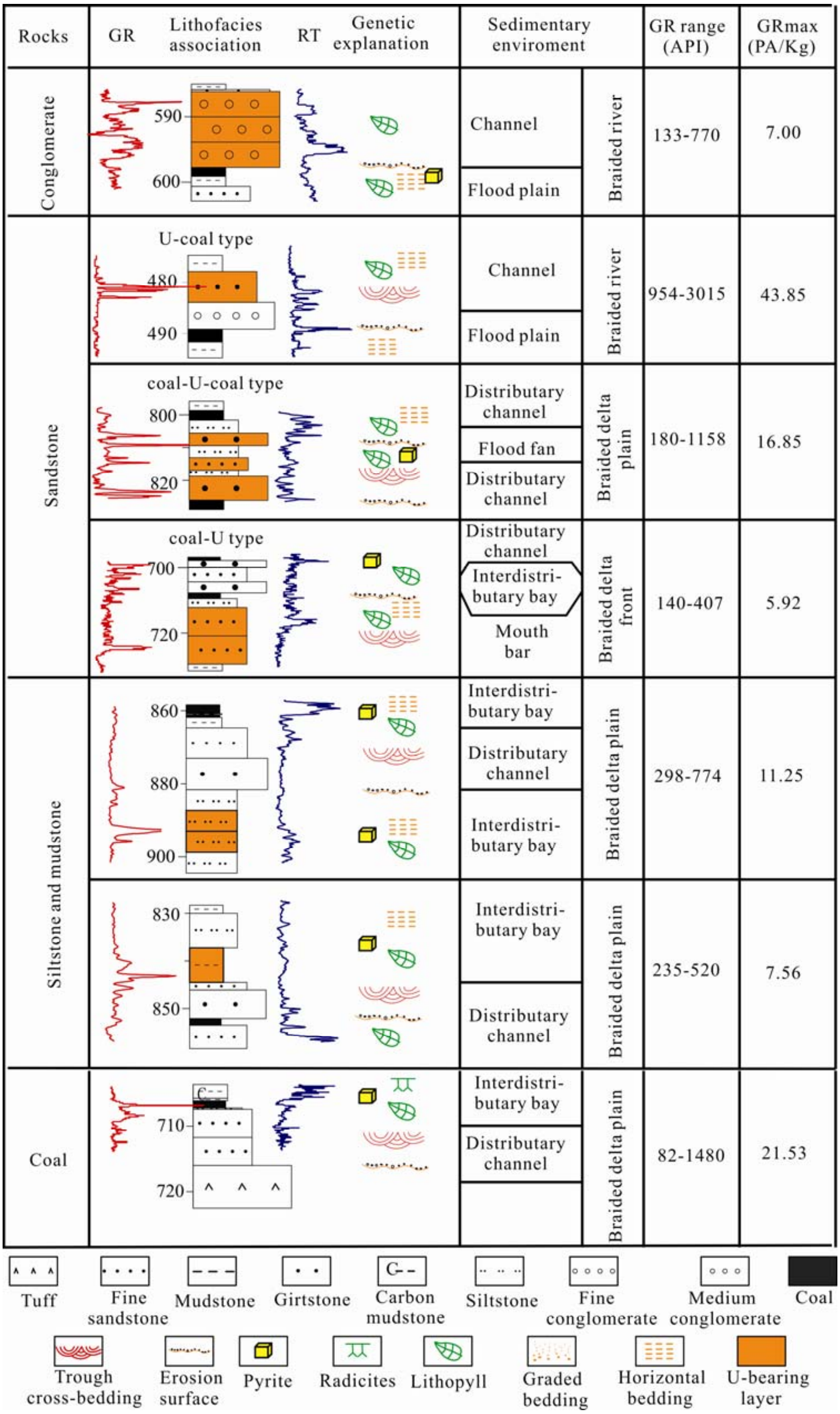

Fig. 4. Uranium-bearing rocks in the northern Qaidam Basin.

These U-bearing sandstones are particularly common along the northeastern margin of the basin. The abnormal response features of Type 1 sandstone on the gamma ray log are relatively higher (ranging from 954 to 3015 API, GRmax = 43.85 PA/kg) (Fig. 4). However, the distribution of Type 1 U-bearing sandstones is also narrow, only

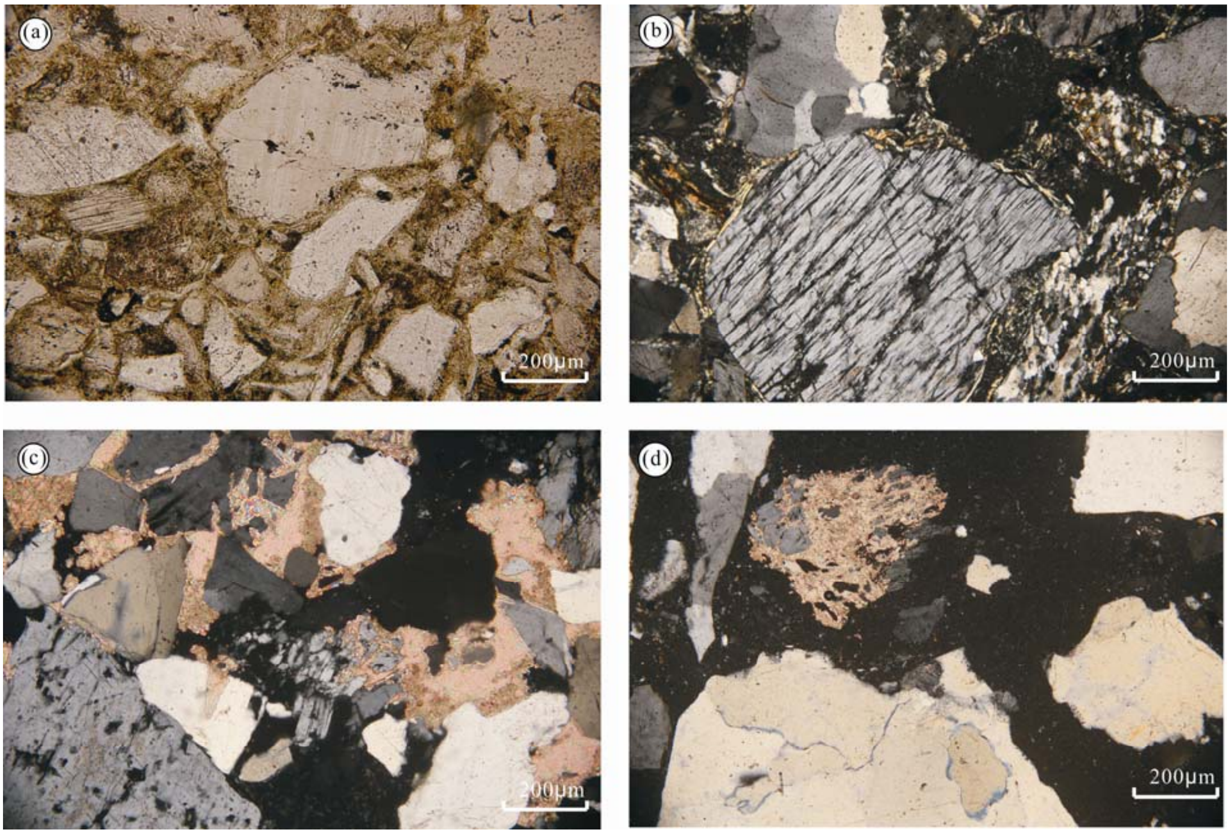

Fig. 5. Epigenetic alteration in the Tuanyushan uranium deposit.
(a), Chloritization, filled between the particles, plane-polarized light, in Type 1 U-bearing sandstones; (b), Sericitization, distributing around the feldspar, cross-polarized light, in Type 1 U-bearing sandstones; (c), Carbonation, filled between the particles, cross-polarized light, in Type 2 U-bearing sandstones; (d), Carbonation, metasomatic feldspar, cross-polarized light, in Type 2 U-bearing sandstones.

occurring at the northeastern margin of the basin in this area.

(2) Type 2 U-bearing sandstone

This type of U-bearing sandstone represents the sandstone that is interbedded by coal (coal-U-coal type), and it mainly occurs in the facies association, very similar to the Type 1, which consists of scour-based, directional conglomerate, trough cross-bedding sandstone, and horizontal-bedding mudstone or coal (Figs. 3b, 3c and 3g). The main differences of Type 2 from the Type1 are as follows: 1) The basal fine conglomerates or conglomeratic sandstones are thinner and medium- to well-sorted, and the clasts are better psephicity than those in Type 1; 2) The predominant trough cross-bedding sandstones are medium- to well-sorted and thicker than those of the Type 1, with interbeds of poorly-sorted fine sandstone and carbonaceous mudstone or coal. Coalified plant stems and fragments are common within this facies association. The paleogeography data from the study area reveal that this facies association consistently displays a temporary and spatial relationship with Type 1, which is characterized by vertical superposition and lateral continuity in the paleogeographic map (Li et al., 2014; Shao Longyi et al., 2014). Carbonatization also exists in this type of sandstone (Fig. 5d). The U-bearing sandstones in the Type 2 are widespread in the study area, and are high concentrations of uranium (up to 70 ppm) (Fig. 4).

(3) Type 3 U-bearing sandstone

This type of U-bearing sandstone mainly represents the sandstone that is overlain by the coal (coal-U type), and it occurs in the lithofacies association, which is made up of basal mudstone, thick well-sorted, trough cross-bedding sandstone interbedded with carbonaceous mudstone or coal, along with scour-based, directional conglomerates, and cross-bedding sandstone from the bottom to the top (Figs. 3d and 3f). The predominant motif shows an upward-coarsening cycle, which ranges from 4 to 30 m in thickness. The basal mudstones contain abundant plant fossils (e.g., plant stems and leaves) with developed laminated or rippled structures (Fig. 3h) turn into siltstone and sandstone interbeds upwards. The proportion and thicknesses of the sandstone interbeds increase upwards in cycles that are characterized by thick, well-sorted, fine- to medium sandstone. This type of sandstone is known to be rich in uranium (up to 35 ppm), and this type of sandstone contains small-medium scale trough cross beds. The top lithofacies consist of associations of coal or carbonaceous mudstone, scour-based conglomerate, and cross-bedding sandstone. This facies association represents a close genetic connection with the Type 2, which may be reflected on the lateral and vertical successions between them.

4.1.3 Fine siliciclastic rock and coal

The fine siliciclastic rocks, such as siltstone and mudstone, in the northern Qaidam Basin are also rich in uranium (GRmax=11.25 PA/kg, 800 API) (Figs. 3f and 4). These rocks contain abundant organic matter and are usually adjacent to the sandstone and conglomerate. Lots of mudstones or siltstones rich in uranium can be found around the Type 1, 2, 3 sandstones.

The concentration of uranium in coal has been determined to range from 0.5 to 10 ppm (Swaine, 1990; Dai et al., 2015), and it is estimated to be up to 2.9 ppm on average for globally low-ranked coal (Ketris and Yudovich, 2009). The average uranium concentrations for common Chinese and US coal are 2.43 and 2.1 ppm, respectively (Finkelman, 1993; Dai et al., 2015). Although fewer data have been made available regarding the uranium in coal, the present study has found that coal in the northern Qaidam Basin contains high concentrations of uranium (up to 16 ppm and higher).

4.2 Geochemistry

4.2.1 Trace elements and organic matter

Table 1 presents the uranium content and accompanying elements in rocks with different content of organic matter. The uranium content in coal samples ranged from 6.2 to 18.7 ppm; it may be lower in other cores from the north Qaidam Basin that were previously measured by other researchers (Wang Dan, 2015). In comparison with the coal samples in this study area, the uranium content in the fine siliciclastic sediments, such as mudstone, silt mudstone or carbonaceous mudstone, takes on an irregular change across the entire area. In some cores, mudstone can contain more than 30 ppm of uranium, equivalent to the industrial utilization value; however, the mudstones close to these U-rich mudstones, only contain less than 2 ppm of uranium. In this study, the fine siliciclastic sediments were only sampled in the predicted U-rich zone. The uranium content in the fine siliciclastic sediments ranged from 3.7 to 10.3 ppm. Meanwhile, the organic geochemistry measured in these rocks showed a relationship between the uranium and organic matter content. Acid hydrolytic hydrocarbon and gas chromatographic analyses were conducted on uranium-bearing sandstones from three wells in order to identify the hydrocarbons. As shown in the Table 2, CH_4 is the main acidolysis hydrocarbon in the U-bearing bed. Further the acidolysis hydrocarbon content appeared to increase with an increase in the U-content in the sandstones.

4.2.2 C-O isotopes of carbonate cement in the U-bearing sandstones

As shown in Table 3, the $\delta^{18}O$ ranged from −17.3‰ to −11.2‰ in the study area, with an average of −14.29‰, $\delta^{18}O_{SMOW}$ ranged from 13.03‰ to 19.32‰, and the $\delta^{13}C$ ranged from −16.9‰ to −1.8‰, with an average of −10.25‰ in carbonate cement in the U-bearing sandstones.

Table 1 Analysis of uranium and accompanying elements in rocks in the Tuanyushan area

Borehole	Sample	Organic geochemistry (%)		Uranium and accompanying elements (ppm)					
		TOC	Chloroform "A"	U	Th	V	Mo	Re	Se
Zku-1	Coal 1	29.05	0.19	16.4	13.7	218	18.5	0.083	2.09
	Coal 2	35.21	0.26	13.3	19.7	227	12.3	0.083	1.92
	Coal 3	32.14	0.16	18.7	11.2	198	15.3	0.082	0.82
Zku-2	Coal 1	13.26	0.06	6.2	29.8	248	6.4	0.083	0.74
	Coal 2	26.31	0.17	14.2	21.3	239	15.3	0.082	1.88
Zku-3	Coal 1	33.21	0.22	15.6	23.4	243	17.3	0.082	1.99
	Coal 2	30.78	0.14	15.2	22.5	223	14.5	0.082	1.65
	Coal 3	25.43	0.16	14.8	10.8	212	10.1	0.082	1.86
	Coal 4	22.13	0.34	16.2	9.7	238	15.0	0.081	0.91
Zku-1	Carbon mudstone	11.81	0.03	5.4	6.3	88	1.4	0.082	0.69
	Mudstone 1	3.22	0.07	10.3	5.4	106	3.7	0.082	0.43
	Mudstone 2	1.43	0.22	4.3	18.7	154	4.6	0.081	0.70
Zku-2	Mudstone 1	6.17	0.56	5.8	21.6	182	5.9	0.082	0.8
	Mudstone 2	5.30	0.42	8.9	20.1	203	7.4	0.081	0.75
	Mudstone 3	9.3	0.54	3.7	22.7	186	2.7	0.080	0.67
Zku-3	Silt mudstone	0.42	0.25	4	23.2	115	0.7	0.081	0.17
	Mudstone 1	2.13	0.17	3.7	22.1	153	1.2	0.082	0.20
	Mudstone 2	6.2	0.39	4.9	24.1	177	4.7	0.082	0.36

Table 2 Analysis of acidolysis hydrocarbon in the U-bearing beds, Tuanyushan area

Sample, U-content and (sample number)	Acidolysis hydrocarbon content (μL/kg)						
	CH_4	C_2H_6	C_3H_8	iC_4H_{10}	nC_4H_{10}	iC_5H_{12}	nC_5H_{12}
Sandstones, w(U)<0.003%, (7)	146.12	25.21	18.63	1.44	3.61	1.49	1.57
U-bearing sandstones, w(U)=0.003%–0.005%, (6)	166.89	33.31	15.39	2.01	1.71	0.59	0.69
Uranium ore, w(U)>0.005%, (7)	292.23	79.42	34.45	3.68	8.01	2.86	2.45

Table 3 Results of C-O isotopes of carbonate cement from U-bearing sandstones from Tuanyushan area

Borehole	Depth(m)	Position	Lithology	$\delta^{13}C_{PDB}$(‰)	$\delta^{18}O_{PDB}$(‰)	$\delta^{18}O_{SMOW}$(‰)
zku-1	810.3	J2	medium sandstone	−14.6	−13.8	16.63
zku-1	812.6	J2	fine sandstone	−13.7	−12.8	17.67
zku-1	814.7	J2	fine sandstone	−16.1	−17.3	13.03
zku-1	815	J2	siltstone	−12.6	−12.3	18.18
zku-2	910.2	J2	siltstone	−9.7	−11.2	19.32
zku-2	913.4	J2	siltstone	−3.9	−12.8	17.67
zku-2	914.5	J2	siltstone	−5.7	−15.6	14.78
zku-2	920.9	J2	gritstone	−1.8	−14	16.43
zku-3	1000.2	J2	Fine sandstone	−10.3	−13.9	16.53
zku-3	1001.4	J2	Fine sandstone	−9.8	−16.6	13.75
zku-3	998.9	J2	Medium sandstone	−16.9	−15.8	14.57
zku-3	1002.3	J2	gritstone	−7.9	−15.4	14.99

4.3 Uranium concentrations in sedimentary rocks of different facies

4.3.1 Braided rivers

As described in section 4.1.1, the conglomerate-dominated, upward-fining cycles with basal erosional surfaces are interpreted as the typical gravel-dominated braided river facies (Cant and Walk, 1976; Miall, 1985; Miall and Jones, 2003; Bridge, 2006). The imbricate arrangements and basal erosional surfaces represent the channel elements described by Miall (1985). The channel elements consist of basal conglomeratic channel lags, which were developed during the periods of peak discharge, and the fining-upward cycles were formed during the period of weakened discharge (Williams and Rust, 1969; Bridge and Tye, 2000). The facies association of Type 1 U-bearing sandstone including the sandstone-dominated, upward-fining cycles with basal scour surfaces is also interpreted as the sandy-dominated braided river facies, which is analogous to the gravel-dominated braided river described above.

The braided river deposits in the northern Qaidam Basin predominantly occurred in the southern region of the Saishiteng−Lvliangshan−Olongbuluke Mountains. The U-coal type sandstone occurs primarily in this sedimentary environment. Although some fine siliciclastic sediments are also rich in uranium, the distributions are too narrow to be exploited. The uranium-bearing rocks consist of the previously described conglomerates and coarse sandstones, which are interpreted as braided river channel deposits. The U-rich sandstones or conglomerates sit above the coal or mudstones and are overlain by mudstones whose source is interpreted as flood plains. These facies show apparent abnormities of natural gamma, which ranges from 100 to 3,015 API (GR_{max}=43.85 PA/kg). However, the average U-content in these facies is low (only up to 27.54 ppm) (Fig. 6; Table 4).

4.3.2 Braided river delta

Braided river deltas are widely distributed in the Middle Jurassic, and in the northern Qaidam Basin, they are the most important coal forming environments; they have been determined to be the main uranium-bearing facies regionally (Zhang Jindai et al., 2008, 2012; Wang Dan et al., 2015). Generally, the most favorable uranium-bearing sedimentary microfacies are the distributary channels in braided river delta plains and the mouth bars in delta fronts.

The facies association, of Type 2 U-bearing sandstones, characterized by the sandstone-dominated, upward-fining cycles with basal scour surfaces is interpreted as typical of sandy-dominated braided river or deltaic distributary channel deposits (Miall, 1985; Miall and Jones, 2003). The temporary and spatial connection between Type 1 and Type 2 and the minable coal beds at the top of this facies indicate that the Type2 should be interpreted as the deltaic distributary channel deposits. The channel elements consist of basal conglomeratic channel lags and fining-upward U-bearing sandstones. The interbed of the poorly-sorted fine sandstone could be regarded as a flood fan formed during the period of peak discharge. The lithofacies at the top, consisting of coal and carbonaceous mudstone, is interpreted as floodplain or inter-distributary bay deposits which are the main coal-accumulating environments in the northern Qaidam Basin.

The distributary channel deposits are connected with the upstream braided river channel and are vertically constricted by inter-distributary bay deposits. The inter-distributary bay deposits not only provide the stable water-resisting layers enabling the formation of the typical U-rich lithological association (coal-U-coal) in this area, but also directly absorb a small amount of uranium (Wang Dan et al., 2015). The sandstones in this type of facies are characterized by an excellent connectivity and stratification, which are favorable for the flow of U-rich fluids. In this area, this type of sandstone has high concentrations of uranium (up to 70 ppm), and is considered the main source of U for extraction (Fig. 7; Table 5). The braided river delta plain, as the main coal-forming environment in the study area, is characterized by an association of the coal-uranium deposits.

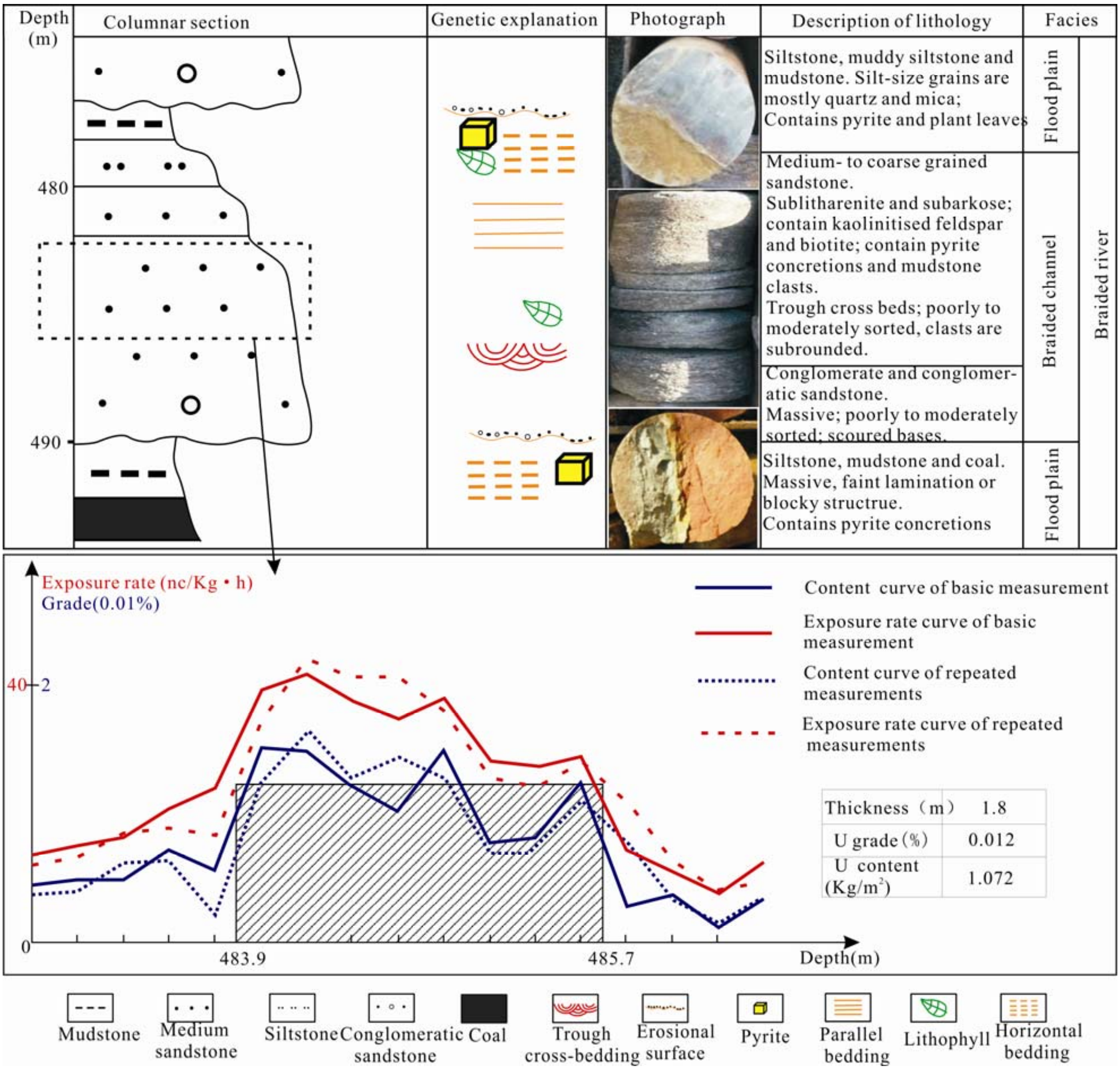

Fig. 6. Braided river and uranium anomaly horizon and Gamma well-logging interpretation.

Table 4 U content and chemical analyses of the braided river deposits

Sample No.	U-Ra equilibrium and U content analyses				Complete chemical analyses				
	U (ppm)	^{226}Ra (10^{-11}g/g)	Th (ppm)	K(wt%)	SiO_2 (wt%)	Al_2O_3 (wt%)	Fe_2O_3 (wt%)	FeO (wt%)	CaO (wt%)
Zk8-23-1	15.67	0.463	6.39	1.41	87.32	5.52	0.652	0.943	0.465
Zk8-23-2	12.75	0.362	25.53	1.82	55.74	23.29	3.84	0.404	0.555
Zk11-18-1	5.74	0.37	9.76	1.56	52.32	8.5	0.853	0.843	16
Zk11-18-2	27.54	0.748	6.43	1.39	83.16	5.87	1.27	1.06	2.04

The Type 3 sandstones, characterized by upward-coarsening cycles, could be interpreted as a braided river deltaic deposit. The basal laminated or rippled mudstone, rich in plant fossils, is regarded as prodelta mudstones, which can be recognized in a few wells in this area. The thick, well-sorted, trough cross-bedded sandstone is interpreted as a delta front mouth bar deposit. The top unit is interpreted as a delta plain facies, which is similar to the Type 2 U-bearing sandstone. According to the sedimentary micro-facies distribution, the mouth bars are laterally connected with distributary channels in its upstream direction, and they are vertically interbedded between the mudstones of the inter-distributary bay and prodelta. These depositional structures also have the sand bodies with good connectivity and interlamination fluidity that are conducive to epigenetic mineralization (Fig. 8;

Table 5 U content and chemical analyses of the braided delta plain deposits

Sample No.	U-Ra equilibrium and U content analyses				Complete chemical analyses				
	U(ppm)	^{226}Ra(10^{-11}g/g)	Th(ppm)	K(wt%)	SiO_2 (wt%)	Al_2O_3 (wt%)	Fe_2O_3 (wt%)	FeO (wt%)	CaO (wt%)
Zku-1-1	18.53	0.334	4.39	1.32	82.45	6.23	0.932	0.712	0.322
Zku-1-2	12.72	0.325	24.44	2.08	57.39	24.32	1.65	0.564	0.460
Zku-1-3	35.07	1.14	17.30	2.09	66.12	18.07	2.22	0.720	0.612
Zku-1-4	29.56	0.438	4.56	1.43	84.02	6.72	1.89	1.24	2.46
Zku-2-1	57.02	2.39	13.76	2.13	69.15	15.06	1.82	0.676	2.11
Zku-2-2	53.21	2.02	22.65	2.22	57.32	25.34	1.45	0.642	0.82
Zku-2-3	40.52	1.22	20.08	1.90	68.65	8.24	1.67	0.675	6.8

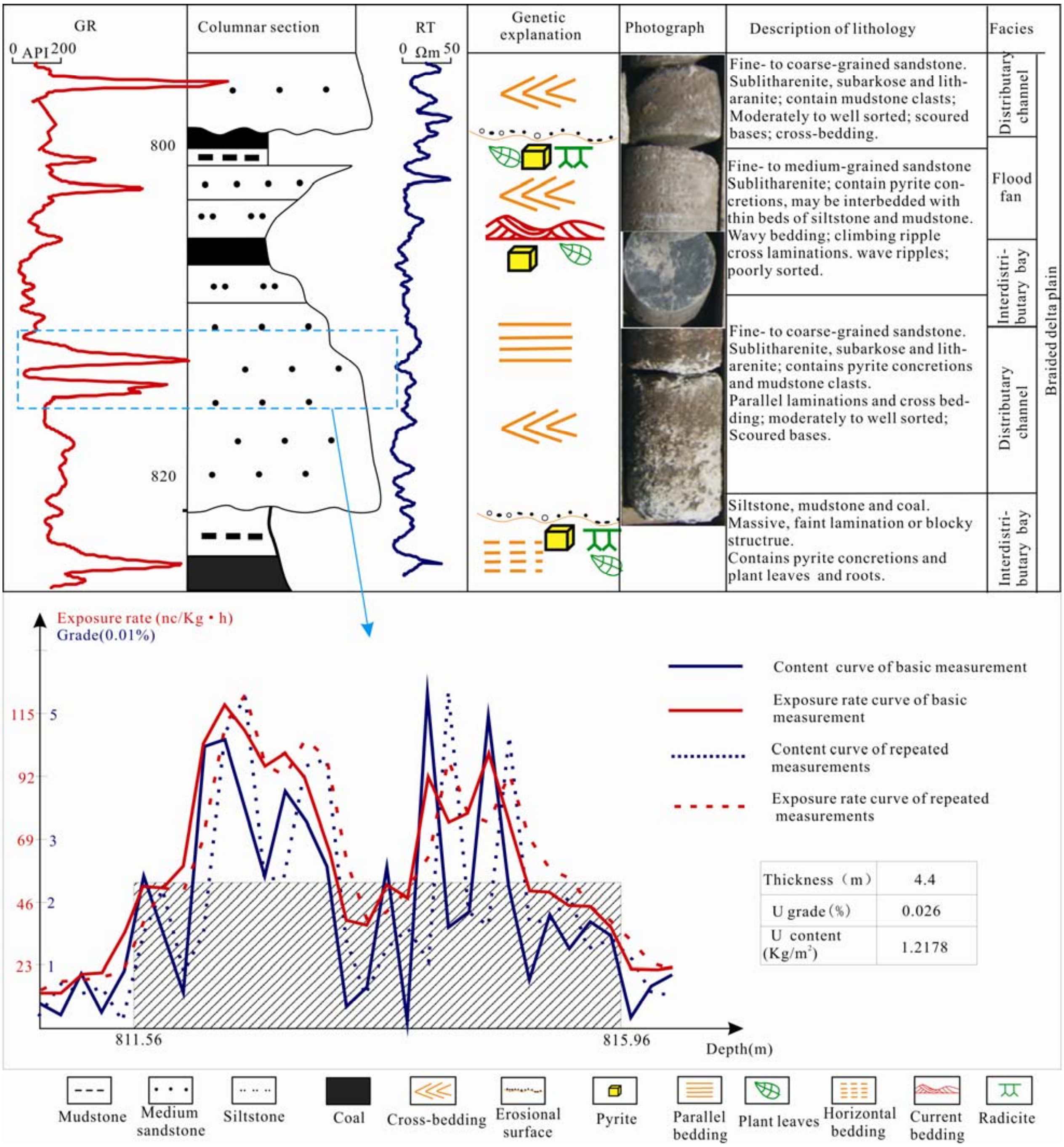

Fig. 7. Braided delta plain and uranium anomaly horizon and Gamma well-logging interpretation.

Table 6). The mouth bar deposits represent high concentrations of uranium as found in some of the wells (up to 52 ppm), and they have been considered as a minor source of U for extraction in this area.

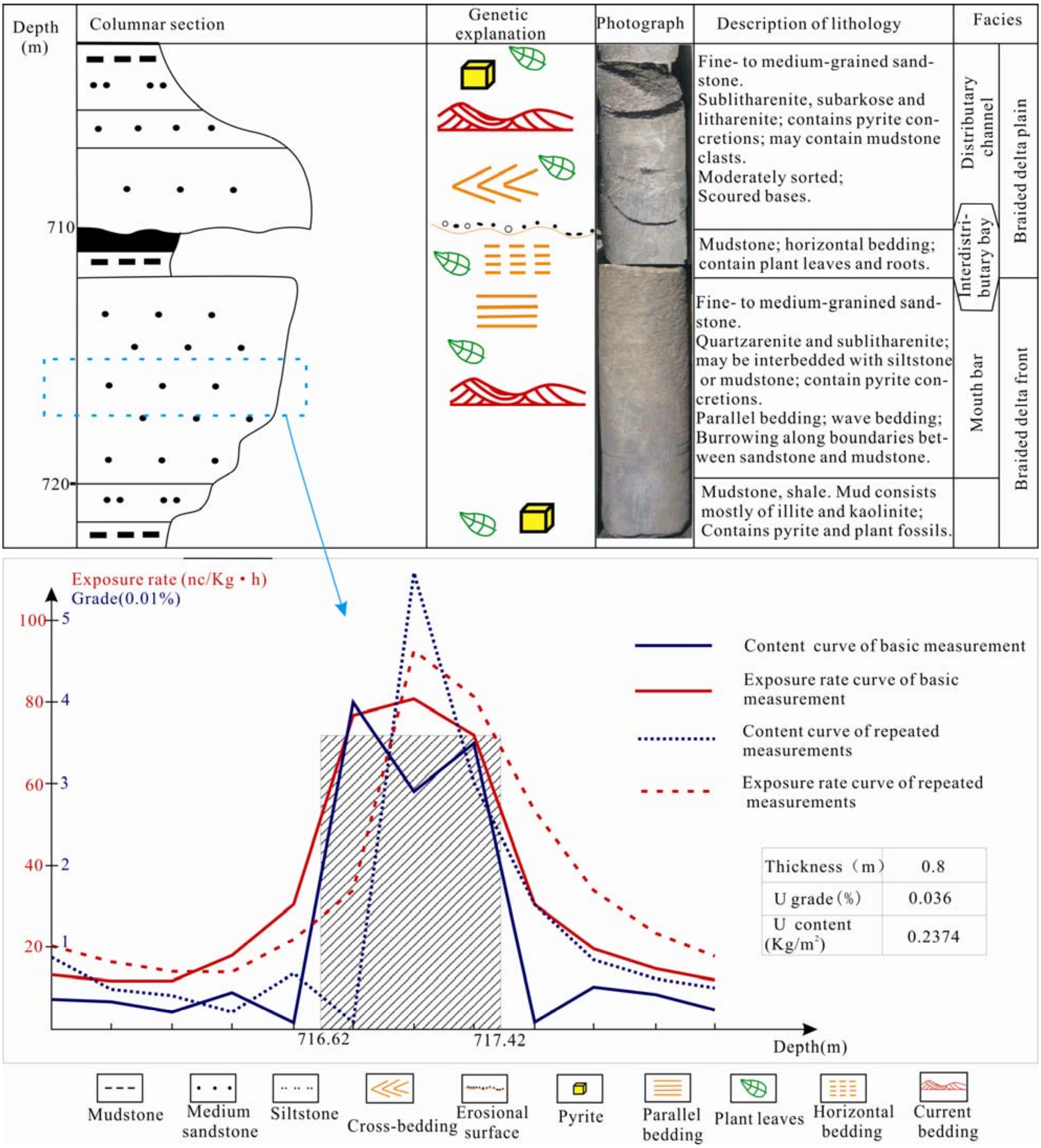

Fig. 8. Braided river delta front and uranium anomaly horizon and Gamma well-logging interpretation.

Table 6 U content and chemical analyses of the braided river delta front deposits

Sample No.	U-Ra equilibrium and U content analyses				Complete chemical analyses				
	U(ppm)	^{226}Ra(10^{-11}g/g)	Th (ppm)	K (wt%)	SiO_2 (wt%)	Al_2O_3 (wt%)	Fe_2O_3 (wt%)	FeO (wt%)	CaO (wt%)
Zku-3-1	3.37	0.114	6.35	2.12	80.02	7.73	0.562	0.412	3.18
Zku-3-2	32.34	0.832	5.78	2.82	80.16	7.31	1.39	0.338	2.35
Zku-3-3	52.01	1.93	23.76	2.03	75.57	14.19	0.67	0.534	1.75
Zku-3-4	40.91	1.638	9.85	1.45	81.21	4.43	1.56	1.26	2.64

5 Discussions

5.1 Spatial control on the uranium mineralization in the coal-bearing series

The primary difference between sedimentary uranium deposits and other types of uranium ore is that the lithofacies, a geological structure and hydrodynamic condition, are the main governing factors in the mineralization process. For sandstone-type uranium deposits, it is especially important to expound the development characteristics of sand bodies, which include sandstone structure, lateral continuity, and plane distribution. The paleo-environment of the study area shows that the lower Shimengou Formation is composed of braided river delta and lacustrine environments. According to the analysis of the lithology and experimental measurements in the Tuanyushan area, two types of sedimentary facies (braided river and braided river delta) are found to be favorable for the occurrence of uranium deposits, which are also the main coal-forming environments in this area. The braided distributary channels can reach quite a large-scale and are surrounded by the inter-distributary bays. Uranium mineralization is located in the distributary channels and more active near the inter-distributary bays (Fig. 9).

5.1.1 Relationship between skeletal sandstones and uranium in the coal-bearing series

Figure 10 shows the distribution of sandstones and U-rich deposits in the Shimengou Formation. The cross section is oriented approximately north-northwest and parallel to the Olongbuluke Mountains. Uranium-rich deposits mainly occur in the braided river deltas, which are characterized by high sand percentage and a large scale of skeletal sandstone body. These sandstone bodies provide the channel or space for migration of U-rich fluids and uranium mineralization. The U-rich deposits could extend to a large scale in sandstone bodies when the channels were laterally connected with each other. The fine siliciclastic sediments such as mudstones, siltstones or coals form the confining beds which can separate the skeletal sandstone bodies into several isolated units and define the location of uranium mineralization. Figure 11 shows the distribution of sedimentary facies, which is approximately perpendicular to the Olongbuluke Montains. In this section, the sedimentary microfacies distribution and sedimentary evolution during the Middle Jurassic are clearly visible. Landward, the distributary channels of the braided river delta plain are well developed with thick sandstones and a higher sandstone-stratum ratio. Towards the basin, the sedimentary environment gradually turns into shallow lakes with thin sandstones and a lower sandstone-stratum ratio. The U-rich deposits still occur in the channel sandstone bodies and extend into the basin. The scale of the skeletal sandstones can control the mineralization potential, which is in direct proportion to the scale of the sandstone bodies (Jiao et al., 2005). Finer-grained sediments are unsuitable for the development of uranium mineralization. Therefore, the U-rich deposits can be gradually wedged out with the change in the depositional facies, which can be shown as the confluence of several ore-bearing fluids or the discontinuous flow units confined by the fine sediments.

The porosity and permeability of sandstone bodies, which vary with the sedimentary microfacies, are also related to the rate of uranium mineralization. The U-rich sandstones occurring in the braided river facies have a

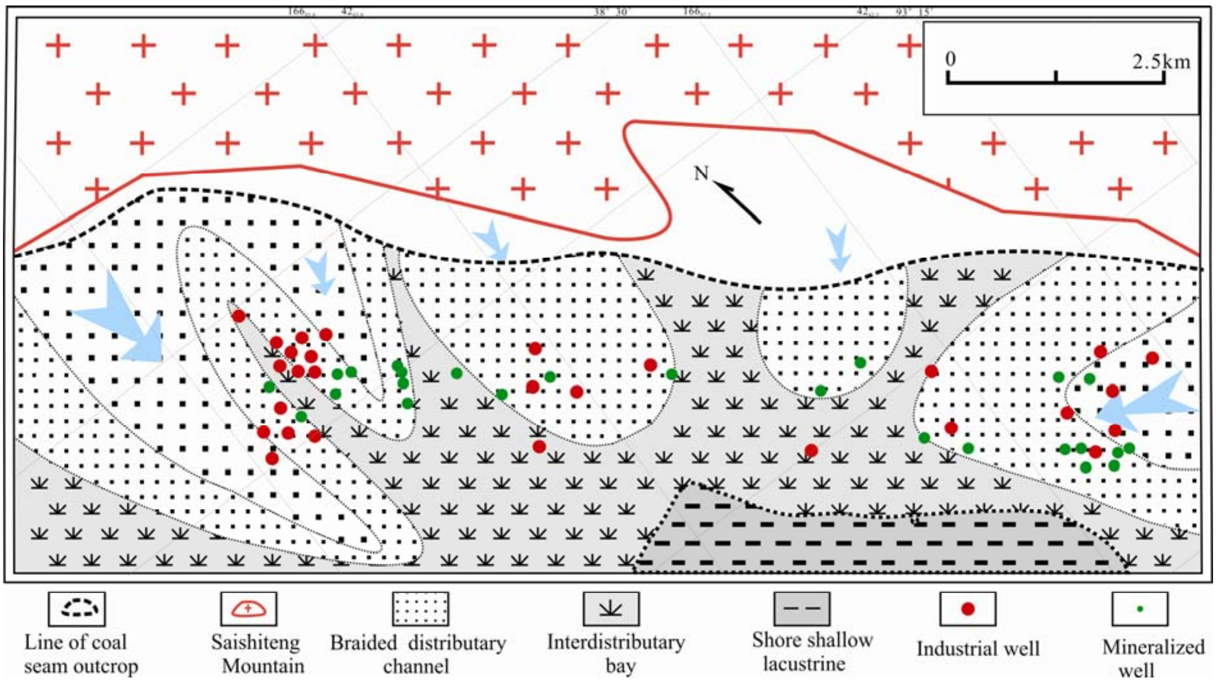

Fig. 9. Paleo-environmental map and locations of mineralized wells in the Tuanyushan area.

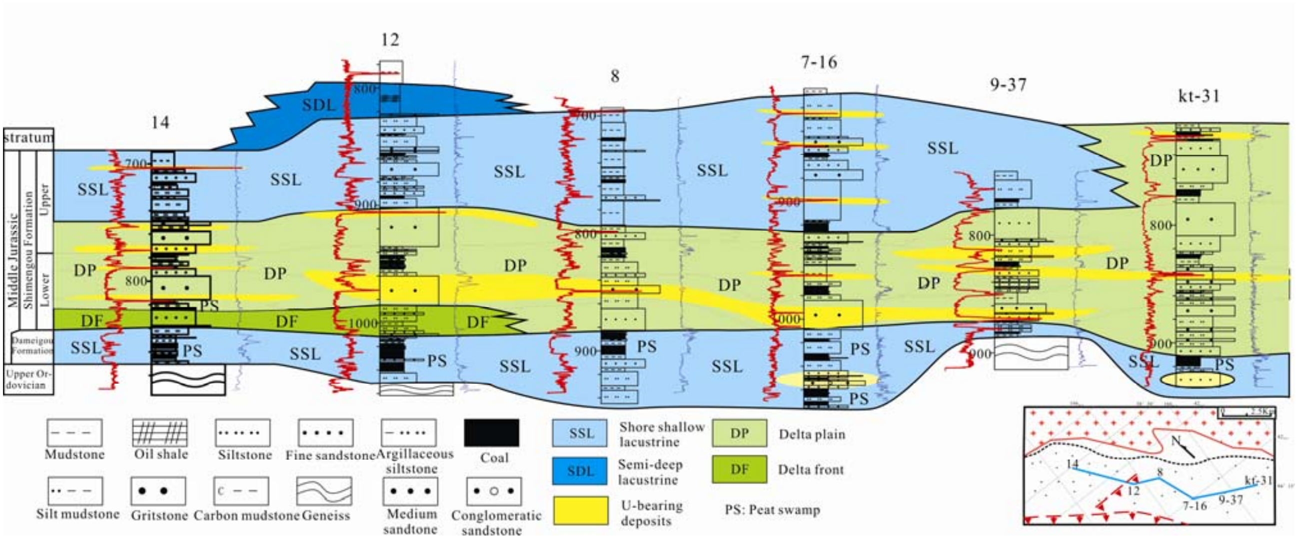

Fig. 10. Correlation cross section A and the sedimentary interpretation of the Shimengou Formation in the Tuanyushan area. The lithological columns are associated with gamma ray logs (red) and the apparent resistivity logs (purple).

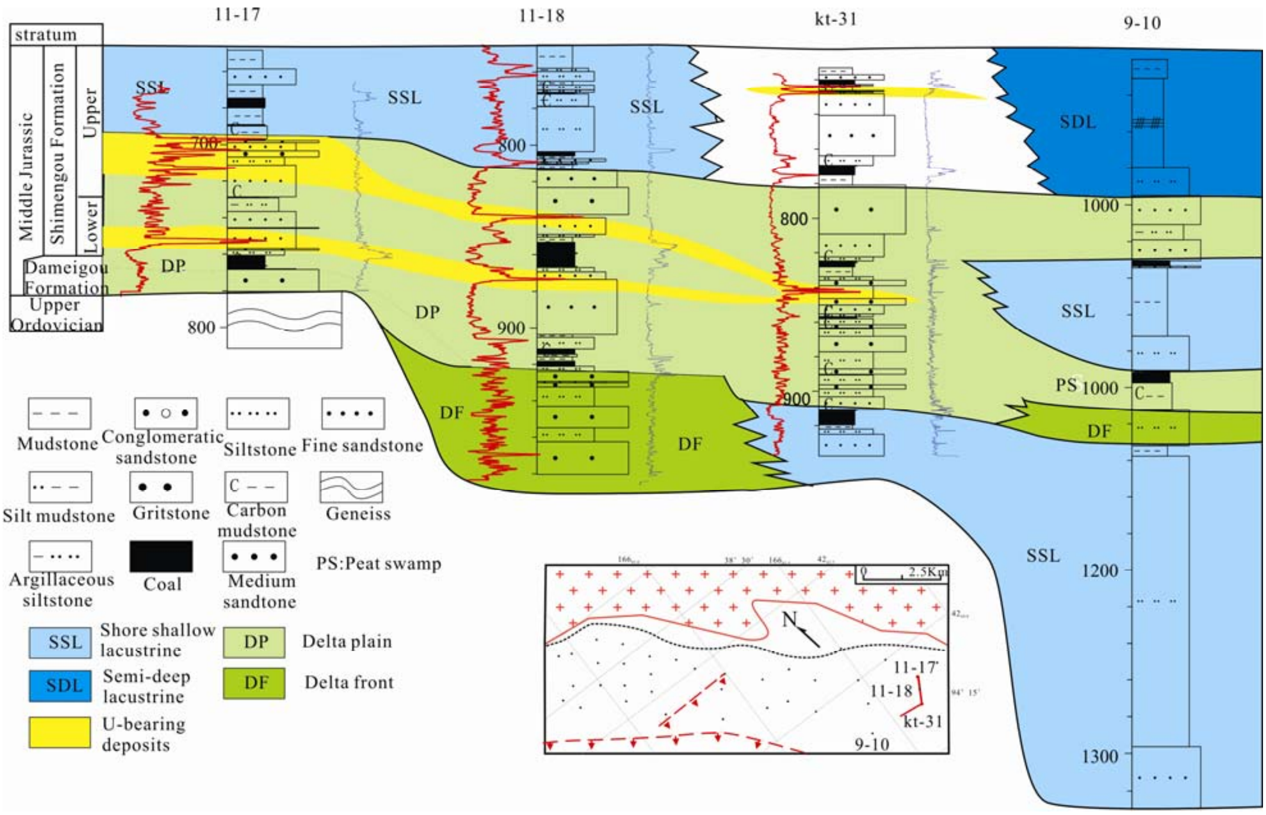

Fig. 11. Correlation cross section B and the sedimentary interpretation of the Shimengou Formation in the Tuanyushan area. The lithological columns are associated with the gamma ray logs (red) and the apparent resistivity logs (purple).

porosity of more than 21.2% and an average permeability of 0.086 μm^2. In the braided river delta facies, the sandstones with porosity of around 25.31% and permeability of around 0.176 μm^2 are the best uranium reservoirs. These differences in reservoir quality may be caused by the shale content in the sandstone and the spatial structure of sandstone and coal.

5.1.2 Relationship between coal and uranium in the coal-bearing series

It can be concluded that the physical conditions and spatial distribution of sandstones in the coal-bearing series have an important role to play in the process of uranium mineralization and concentration. After the analysis of lithological association and paleogeography, it can be reckoned that uranium mineralization always occurs in the skeletal sandstones that have close relationships with coal, such as U-coal, coal-U or coal-U-coal types described as above.

Figure 12 shows the sandstone and coal isolith of the lower Shimengou Formation in the study area. The industrial or mineralized wells were regularly found in coal-bearing regions with the coal amounting to more than 10 m in thickness. There are coal seams over or under the uranium deposits in the section with a vertical distance of 0−10 m. The changes in thickness of the uranium deposits also respond well to that of the coal seams (Wang, 2015). The coals can act as confining beds preventing the U-rich fluids from infiltrating and enabling them to migrate within the skeletal sandstones. In addition, as described above, U-rich coals can also be found in this area. However, not all of the coal of the Tuanyushan area is rich in uranium. Only the coal adjacent to the sandstone-type uranium deposits can be enriched in uranium. Danchev and Strelyanov (1979), Seredin and Finkelman (2008), and Dai et al. (2015) argued that the uranium deposits hosted in coal, generated by epigenetic infiltration, showed a zoned distribution. The optimal uranium-bearing zone (Zone 1), directly underlying the sandstone and behind the fluid front, usually contains oxidized coal enriched in inertinite (e.g., fusinite or semi-fusinite) and Fe hydroxides (Seredin and Finkelman, 2008; Dai et al., 2015), and that the uranium in Zone 1 mainly occurs in its hexavalent form in the organic matter (Seredin and Finkelman, 2008). The uranium-bearing Zone 2, under Zone 1, is prominently mineralized and has a high content of pyrite and other epigenetic selenides or sulfides. Different from Zone 1, the uranium in Zone 2 mainly occurs in its tetravalent form U(IV) in oxides and silicates (e.g., coffinite or pitchblende) (Seredin and Finkelman, 2008; Dai et al., 2015). Low uranium concentrations occur in unaltered coal underlying the front zone. The highest concentrations of uranium are located in the upper zones around the contacts with the oxidized host sandstones and also in the front zone at certain distances from the oxidized rocks (Dai et al., 2015).

5.2 Dynamic control on uranium mineralization in the coal-bearing strata

Research has shown a close spatial relationship between the uranium-bearing rocks and coal or fine siliciclastic sediments; however, assuming this as the main contributing factor for the concentration of uranium in the coal-bearing series is still not ascertained. A profound study should shed light on the internal factors as the main drivers explaining why most of U-rich deposits occur in coal-bearing series.

Coal and organic matter in the coal-bearing series are kinds of reductants, which can serve as good reducing and absorbing barriers (Spirakis et al., 1996; Wu Bolin et al., 2006). Along with epigenetic sulfides and selenides, they can dynamically control the uranium deposits during the period of mineralization.

As shown in Table 1, there is a positive correlation between the content of organic matter and uranium in the U-bearing rocks (with the exception of the sandstones). The results from the Tuanyushan area are similar to prior research involving the relationship between the uranium and organic matter, which was mainly interpreted as the absorption of uranium to organic matter (Wang et al., 2015). As for this, either coal and fine siliciclastic

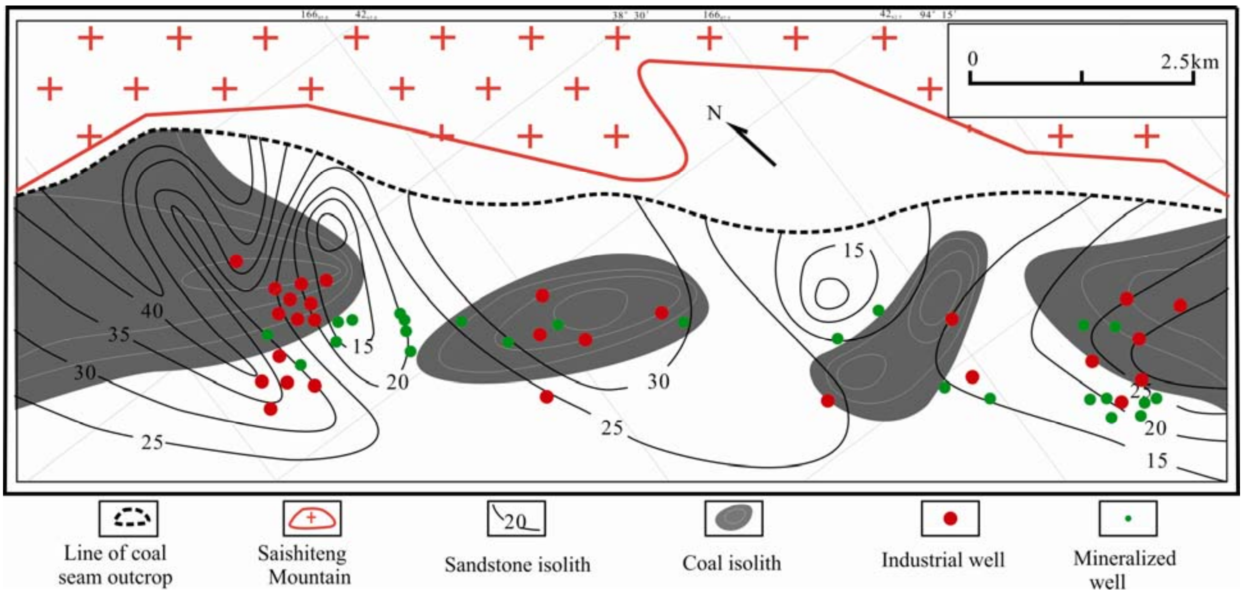

Fig. 12. Sandstone and coal isoliths and location of mineralized wells in the Tuanyushan area.

sediments such as siltstone and mudstone (rich in organic matter), or the sandstone can be described as the uranium reservoirs. It may be reasonable to assume that the different uranium contents in coal and fine siliciclastic sediments are due to the organic matter content; however, the conclusion of sandstone's suitability for U-concentration is incomplete. Table 2 shows that CH_4 is the main acidolysis hydrocarbon in the U-bearing bed, very analogous to the coalbed methane occurring in the underlying coal, and that the acidolysis hydrocarbon apparently increases with the U-content in the sandstones. It is concluded that CH_4 was the most important reduction agent that turned the U^{6+} into U^{4+}, and precipitated the uranium in the sandstones. It is also suggested that the coal at the bottom provided CH_4 (the organic matter or epigenetic sulfides also play an important role in the uranium mineralization.). Experts have speculated that ground water rich in uranium infiltrated the Jurassic in the north Qaidam Basin and was reduced by the hydrocarbon fluids. The acidolysis hydrocarbon test shows that these hydrocarbon fluids should be coalbed methane provided by the coal at the bottom. Wang (2015) also showed that the epigenetic minerals of the U-bearing sandstone correlate to coalification and that the contents and features of trace elements and REE of coal coincide with that of U-bearing sandstones.

In addition, the formation of the sandstone-type uranium deposits should go through uranium activation, migration and accumulation. There are a series of complicated geochemical processes where the traces of the epigenetic U-bearing fluid effects (epigenetic alteration) could be definitely recognized (Wülser et al., 2011; Rong Hui et al., 2016). As described above, carbonatization, which is common in the study area, may provide useful geological information through the process of uranium mineralization. In nature, carbon reservoirs include organic carbon and carbonate, the former denoted by the reduction of carbon, which is characterized by a deficiency of $\delta^{13}C$, and the latter with the oxidation of carbon rich in $\delta^{13}C$ (Kerridge et al., 1985; Ravenhurst et al., 1989; Macaulay et al., 1993; Mostafa et al., 2001). It has been accepted that the $\delta^{13}C$ in inorganic carbon can range from −4.0‰ to 4.0‰ (Clark and Fritz, 1997; Akhtar et al., 2017; Liu et al., 2017). With increasing temperatures and pressure, the organic matter uses decarboxylate and releases carbon dioxide with a low $\delta^{13}C$, which normally ranges from −35.0‰ to −4.0‰ (Clark and Fritz, 1997; Akhtar et al., 2017; Liu et al., 2017). Therefore, a lower $\delta^{13}C$ reflects the notion organic carbon could be involved in the carbonation of carbonate cement. Dai and Chen (1993) examined the carbon isotopes of methane in China and proposed that, if the $\delta^{13}C$ ranges from −14‰ to −42‰, the carbon should be derived from the coal gas. As shown in Table 3, $\delta^{18}O_{SMOW}$ ranged from 13.03‰ to 19.32‰, which is within the range of sedimentary rocks (Hoefs, 1987; Liu et al., 2017), and the $\delta^{13}C$ ranged from −16.9‰ to −1.8‰, with an average of −10.25‰ in carbonate cements in the U-bearing sandstones. Much experimental data is in the range supporting organic matter decarboxylation (Clark and Fritz, 1997; Akhtar et al., 2017; Liu et al., 2017). It turns out that carbonatation in the U-bearing sandstones could be connected to organic matter in the study area. Based on the work of Shikazono and Utada (1997) and Akhtar et al. (2017), a mechanism of chemical reactions can be proposed as follows:

$$SO_4^{2-} + 2H^+ + CH_2O + H_2 \rightarrow H_2S + CO_2 + 3H_2O$$

The H_2S and CO_2 generated in the above reaction form pyrite and calcite as (H_2S can also be provided by the natural gas),

$$H_2S + Fe^{2+} \rightarrow FeS + 2H^+$$

$$CO_2 + Ca^{2+} + H_2O \rightarrow CaCO_3 + 2H^+$$

Fe^{2+} and Ca^{2+} are derived from iron and calcium minerals of sedimentary rocks.

The organic matter got oxidized, degraded, and decarboxylated; the organic matter released carbon dioxide, which reacted with the calcium provided by the dissolution; finally, it generated calcium carbonate (Shikazono and Utada, 1997; Akhtar et al., 2017; Liu et al., 2017). This process was beneficial to uranium activation and migration. In the case of the Tuanyushan uranium deposits, the source of uranium, from granitic or metamorphic rocks in the Olongbuluke Mountains, is mainly in leachable U(VI) form. From source rocks to host rock, uranium migrates via ground water solution (Sanford, 1994; Akhtar et al., 2017). Ground water, rich in carbonaceous matter, can absorb uranium. While migrating through the U-rich granitic rocks in faults, fissures or shear zones, ground water can absorb more uranium (Doi et al., 1975). When the U-bearing water migrated across the coal-bearing series, uranium was changed from hexavalent to tetravalent form and precipitated from the solution (Turner et al., 1993). During this period, organic matter played an important role in controlling the oxidation-reduction state of uranium mineralization (Spirakis, 1996), which could be driven by coal, humic acids, or even solid bitumen. When the host sandstone contains less organic or epigenetic sulfides, methane or organic acid can migrate upward from underlying coal seams along faults and act as the main reductant for uranium mineralization (Goldhaber et al., 1983; Spirakis, 1996). Uranium migrates in the form of $UO_2(CO_3)_3^{4-}$ and $UO_2(CO_3)_2^{2-}$, which requires the abundant presence of CO_3^{2-} in the water (Nash et al., 1981). These bicarbonate $\{UO_2(CO_3)_2\}^{2-}$ and tricarbonate $\{UO_2(CO_3)_3\}^{4-}$ forms of uranium minerals in different reaction are given as follow:

$$UO_2(CO_3)_2^{2-} + 2H^+ \rightarrow 2HCO_3^- + UO_2^{2+}$$

UO_2^{2+} can be reduced to UO_2 (Ritch et al., 1977),

$$UO_2(CO_3)_2^{2-} + H_2O \rightarrow 2HCO_3^- + UO_2 + 1/2O_2$$

Therefore, along with epigenetic sulfides, the organic matter in the coal-bearing series, whether in the host sandstone or migrated from the coal, acts as a powerful reductant, which closely relates to the uranium deposits occurring in the sandstone or the porous inertinite-rich coal (Dai et al., 2015).

5.3 Dual control of depositional facies on uranium mineralization in coal-bearing series

It is generally accepted that the formation of uranium deposits requires two conditions: (1) sandstone bodies with good connectivity, permeability, and stratification are needed in order to enable the free migration of the U-fluids (Maithani et al., 1995; Polito et al., 2006; Jovan Kovačević et al., 2009; Qiu Yubo et al., 2015); and (2) a confining bed should exist in order to resist permeation and to restrict the mobility of the U-fluid to flow only within the sandstones (Gabelman, 1977; Jiao Yangquan et al., 2015). However, after the interpretation of U-deposit in the Tuanyushan area, uranium mineralization occurring in coal-bearing series takes on more complexity and regularity. As for accommodation, it is essential to provide the reservoir for uranium mineralization in coal-bearing series, which refers to the skeleton sandstones and the porous inertinite-rich coal which not only provided channels for migration of U-bearing fluids but also acted as a reservoir for uranium concentration, and stable confining bed preventing the vertical infiltration of U-bearing fluids. Together, they cause an attempt to enable uranium mineralization occurring in specific space. Importantly, in the coal-bearing series, the coals usually take on close spatial association with the U-deposits, characterized by U-coal, coal-U, and coal-U-coal types. All of these factors work together to generate the innate differences in uranium mineralization between different sedimentary environments. While constituting the stable confining bed and presenting the function of spatial control on U-deposits, the coal (or the organic matter) has a more important role to play in uranium mineralization by acting as the dynamic control that promotes U-concentration. The sandstones, fine siliciclastic sediments, or the coal, can absorb enough uranium amounting to the industrial grades as long as they contain sufficient organic matter. The U-deposits in this area were mainly generated due to the reduction of coal or organic matter in the coal-bearing series. For the reduction in sandstones, CH_4 comes from the bottom, and along with the organic matter or epigenetic sulfides in the host sandstone, reduces the U^{6+} to U^{4+} when the U-rich fluids cross them (Fig. 13①). While in the coal (especially the porous inertinite-rich coal

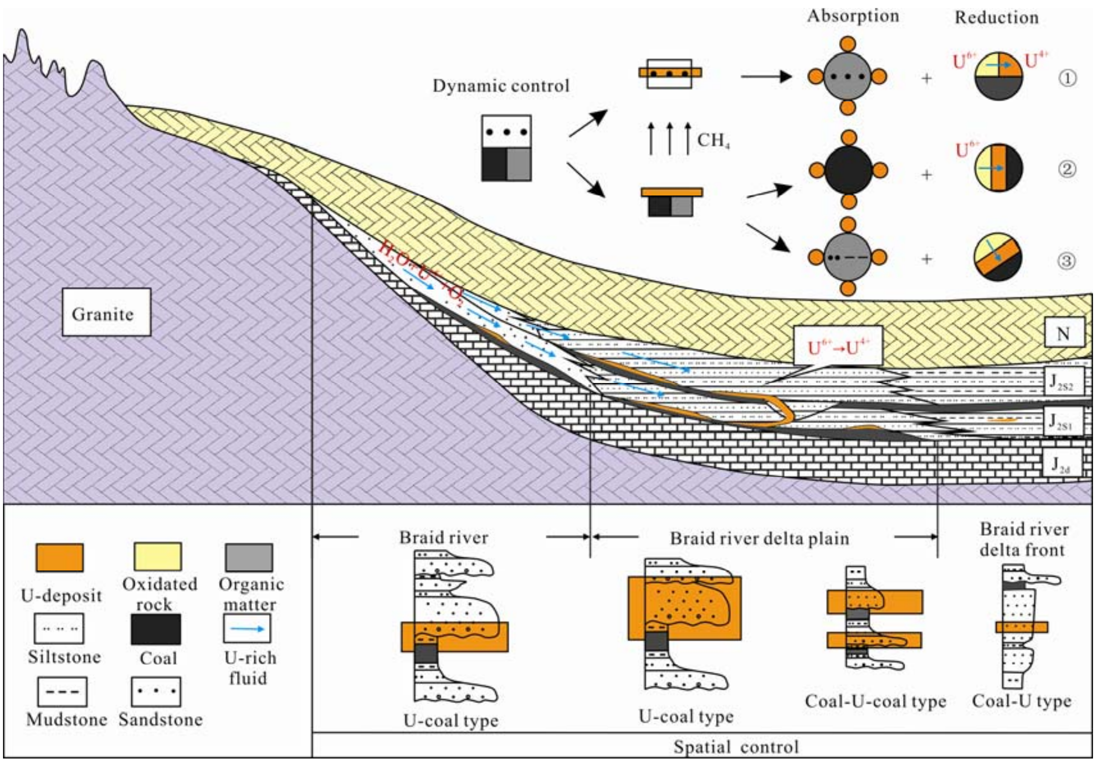

Fig. 13. Dual control of depositional facies on uranium mineralization in coal-bearing series.

not only provided channels for flow of U-bearing fluid but also acted as a reductant), the reduction takes on an apparent zonation characterized by the regular association of trace element composition (Dai et al., 2015) (Fig. 13②). The reduction in the fine siliciclastic sediments can consist of two types (Fig. 13③), which is difficult to recognize, and it may be determined by the content and origin of the organic matter. It is concluded that the dual control of depositional facies in coal-bearing series contributes to the uranium metallogenic tendency and specificity in this area.

6 Conclusions

The uranium deposits are developed in the coal-bearing series in the Tuanyushan area. The effects of depositional facies in the coal-bearing series on the U-deposits represent the dual control including the spatial and dynamic controls which define the metallogenic tendency and specificity in the coal-bearing series.

(1) Five types of uranium-bearing rocks are recognized, and they mainly occur in the braided river and in the braided river delta facies. The sandstones in the coal-bearing series are one of the major sources of uranium for industrial utilization. The lithological association of the braider river delta facies can be subdivided into three types including U-coal type, coal-U-coal type, and coal-U type.

(2) There is a spatial control on the uranium mineralization in the coal-bearing series. The coal-bearing series provide the accommodation for uranium mineralization. The sandstone with fine connectivity and stratification, and porous inertinite-rich coal may influence the quality of the uranium deposits. The lithological association in the coal-bearing series defines the location of metallogeny, whether vertically or laterally, which is bounded by the coal or the fine siliciclastic deposits.

(3) Coal and organic matter in the coal-bearing series act as reductants, which can serve as good reducing and absorbing barriers. They perform the dynamic control on the uranium mineralization. Along with epigenetic sulfides, the organic matter in the coal-bearing series, whether in the host sandstone or migrated from the coal, acts as a powerful reductant, leading to a change in the uranium from hexavalent to tetravalent forms, followed by the precipitation of uranium minerals.

Acknowledgements

This research is supported by the Major National Science and Technology Program of China (grants No. 2016ZX05041004), the National Natural Science Foundation of China (grant No. 41572090) and High-level Talent Recruitment Project of North China University of Water Resource and Electric (grant No. 40481). Many thanks are given to Wang Chongjing and Zhou Kai for their help during sample preparation. Professors Chi Guoxiang and Jiao Yangquan are thanked for their reviews and constructive comments.

Manuscript received Sept. 4, 2017
accepted Dec. 20, 2017
edited by Hao Qingqing

References

Akhtar, S., and Yang, X.Y., 2014. Formation of sandstone-hosted uranium mineralization in the Ordos Basin, Northwestern China, *Acta Geologica Sinica* (English edition), 88(z2): 1337–1345.

Akhtar, S., Yang, X.Y., and Pirajno, F., 2017. Sandstone type uranium deposits in the Ordos Basin, northwest China: A case study and an overview. *Journal of Asian Earth Sciences*, 146: 367–382.

Bostrom, K., 1983. Genesis of ferromanganese deposits–diagnostic criteria for recent and old deposits. In: Rona, P.A., Bostrom, K., Laubier, L., Smith Jr., K.L. (Eds.), Hydrothermal Processes at Seafloor Spreading Centers. Plenum Press, New York, pp. 473–489.

Bostrom, K., Kramemer, T., and Gantner, S., 1973. Provenace and accumulation rates of opaline silica, Al, Fe, Ti, Mn, Ni and Co in Pacific pelagic sediment. *Chem. Geol.*, 11: 123–158.

Bridge, J.S., 2006. Fluvial facies models: recent developments. *Society of Economic Paleontologists and Mineralogists Special Publication*, 84: 85–170.

Bridge, J.S., and Tye, R.S., 2000. Interpreting the dimensions of ancient fluvial channel bars, channels, and channel belts from wireline-logs and cores. *AAPG Bulletin,* 84: 1205–1228.

Cai Yuqi, Zhang Jindai, Li Ziyang, Guo Qingyin, Song Jiye, Fan Honghai, Liu Wusheng, Qi Fucheng and Zhang Minglin, 2015. Outline of uranium resources characteristics and metallogenetic regularity in China. *Acta Geologica Sinica* (English Edition), 89(3): 918–937.

Cai Yuqi, Yi Chao and Zhang Chao, 2014. The geological characteristics and controlling factors of Nalinggou uranium deposits, Northeastern Ordos Basin. *Acta Geologica Sinica* (English Edition): 88(z2): 1339–1340.

Cant, D.J., and Walker, R.G., 1976. Development of a braided-fluvial facies model for the Devonian Battery point Sandstone, Quebec. *Canadian Journal of Earth Science*, 13(1): 102–119.

Chen Daisheng, Li Shengxiang and Cai Yuqi, 2006. Overview of the researches on sedimentary environment for sandstone type uranium deposits in the Meso-Cenozoic basins of China. *Acta Sedimentologica Sinica*, 24(2): 221–228 (in Chinese with English abstract).

Chen Fenxiong, Nie Fengjun, Zhang Chengyong and Zhang Zhanfeng, 2016. Sedimentary facies of the Lower Jurassic Sangonghe Formation and its relationship with uranium mineralization in Mengqiguer area of Yili Basin, Xinjiang. *Journal of Palaeogeography*, 18(5): 833–842 (in Chinese with English abstract).

Clark, I., and Fritz, P., 1997. *Environmental Isotopes in Hydrogeology*, Lewis Publishers, New York, 328.

Dahlkamp, F.J., 1993. *Uranium Ore Deposits*, Springer-Verlag, Berlin, 259–319.

Dai Junsheng, Ye Xingshu, Tang Liangjie, Jin Zhijun, Shao Wenbin, Hu Yong and Zhang Bingshan, 2003. Tectonic units and oil-gas potential of the Qaidam Basin. *Chinese Journal of Geology*, 38(3): 291–296 (in Chinese with English abstract).

Dai Jinxing and Chen Ying, 1993. The characteristics and Identifications of alkane carbon isotope of biogenetic gas in China. *Science in China (Series B)*, 23(3): 303–310 (in Chinese with English abstract).

Dai, S.F., Seredin, V.V., Ward, C.R., Jiang, J., Hower, J.C., Song, X., Jiang, Y., Wang, X., Gornostaeva, T., Li, X., Liu, H., Zhao, L., and Zhao, C., 2014. Composition and modes of occurrence of minerals and elements in coal combustion products derived from high-Ge coals. *International Journal of Coal Geology*, 121: 79–97.

Dai, S.F., Yang, J.Y., Ward, C.R., Hower, J.C., Liu, H.D., Garrison, T.M., French, D., J.M.K., and O'Keefe, 2015. Geochemical and mineralogical evidence for a coal-hosted uranium deposit in the Yili Basin, Xinjiang, northwestern China. *Ore Geology Reviews*, 70: 1–30.

Danchev, V.I., and Strelyanov, N.P., 1979. Exogenic Uranium Deposits. Atomizdat, Moscow (in Russian).

Fan Aiping, Liu Yiqun, Yang Renchao, Feng Qiao, Zhang Fuxin and Han Zuozhen, 2007. Research on diagenesis of the sandstone-type uranium deposits in Dongsheng area, Ordos Basin, *Science in China Series D: Earth Sciences*, 50(Z2): 195–202.

Feng, Z.B., Nie, F.J., Deng, J.Z., Zhang, H.J., and Liu, B.H., 2017. Spatial-temporal collocation and genetic relationship among uranium, coal, and hydrocarbons and its significance for uranium prospecting: A case from the Mesozoic-Cenozoic uraniferous basins, North China. *Russian Geology and Geophsics*, 58: 611–623.

Finkelman, R.B., 1993. Trace and minor elements in coal. In: Engel, M.H., Macko, S. (eds), *Organic Geochemistry. Plenum*, New York, 593–607.

Finkelman, R.B., and Brown Jr., R.D., 1991. Coal as host and as an indicator of mineral resources. In: *Peters, D.C. (Ed.), Geology in Coal Resource Utilization. Fairfax, Techbooks, Virginia,* 471–481.

Gabelman, J.W., 1977. Migration of uranium and thorium-exploration significance. *AAPG*, 173.

Galloway, W.E., and Hobday, D.K., 1983. *Terrigenous Clastic Depositional Systems-Application to Petroleum, Coal and Uranium Exploration*. Springer, New York Heidelberg, 423.

Gayer, R.A., Rose, M., Dehmer, J., and Shao, L.Y., 1999. Impact of sulphur and trace elements geochemistry on the utilization of a marine-influenced coal-case study from the South Wales Variscan foreland basin. *International Journal of Coal Geology*, 40: 151–174.

Goldhaber, M.B., Reynolds, R.I., and Rye, R.O., 1983. Roll of fluid mixing and fault related sulfide in the origin of Ray Point uranium district, south Taxas. *Economy Geology*, 78: 1043–1063.

Hall, S.M., Mihalasky, M.J., Tureck, K.R., Hammarstrom, J.M., and Hannon, M.T., 2017. Genetic and grade and tonnage models for sandstone-hosted roll-type uranium deposits, Texas Coastal Plain, USA. *Ore Geology Reviews*, 80: 716–753.

Hoefs, J., 1987. Stable Isotope Geochemistry. Springer-Verlag, Berlin.

Hou, B.H., Keeling, J., and Li, Z.Y., 2017. Paleovalley-related uranium deposits in Australia and China: A review of geological and exploration models and methods. *Ore Geology Reviews*, 88: 201-234.

Hu, R.Z., Qi, H.W., Zhou, M.F., Su, W.C., Bi, X.W., Peng, J.T., and Zhong, H., 2009. Geological and geochemical constraints on the origin of the giant Lincang coal seam-hosted germanium deposit, Yunnan, SW China: A review. *Ore Geology Reviews*, 36: 221–234.

Huang Jingbai and Huang Shijie, 2005. Regional metallogenic characteristics of China's uranium resources. *Uranium Geology*, 21(3): 129–138 (in Chinese with English abstract).

Jaireth, S., Hoatson, D.M., and Miezitis, Y., 2014. Geological setting and resources of the major rare-earth-element deposits in Australia. *Ore Geology reviews*, 62: 72–128.

Jiao Yangquan, Wu Liqun, Rong Hui, Peng Yunbiao, Miao Aisheng and Wang Xiaoming, 2016. The relationship between Jurassic coal measures and sandstone-type uranium deposits in the Northeastern Ordos Basin, China. *Acta Geologica Sinica* (English edition), 90(6): 2117–2132.

Jiao Yangquan, Wu Liqun, Peng Yunbiao, Rong Hui, Ji Dongmin, Miao Aisheng and Li Hongliang, 2015. Sedimentary-tectonic setting of the deposition-type uranium deposits forming in the Paleo-Asian tectonic domain, North China. *Earth Science Frontiers*, 22(1): 189–205 (in Chinese with English abstract).

Jiao, Y.Q., Yan, J.X., Li, S.T., Yang, R.Q., Lang, F.J., and Yang, S.K., 2005. Architectural units and heterogeneity of channel reservoirs in Karamay Formation, outcrop area of Karamay oilfield, Junggar Basin, northwest of China. *AAPG Bulletin*, 89: 529–545.

Jin Zhenkui, Qi Congwei, Xue Jianqin, Wang Chunsheng and Fan Xiaona, 2006. Sedimentary facies of the Jurassic in northern margin of Qaidam Basin. *Journal of Palaeogeography*, 8(2): 199–210 (in Chinese with English abstract).

Jovan Kovačević, Zoran Nikić, and Petar Papić., 2009. Genetic model of uranium mineralization in the Permo-Triassic sedimentary rocks of the Stara Planina eastern Serbia. *Sedimentary Geology*, 219: 252–261.

Kerridge, J.F., 1985. Carbon, hydrogen and nitrogen in carbonaceous chondrites: abundances and isotopic compositions in bulk samples. *Geochimca et Cosmochimica Acta*, 49: 1707–1714.

Ketris, M.P., Yudovich, and Ya, E., 2009. Estimations of Clarkes for carbonaceous biolithes: world average for trace element contents in black shales and coals. *International Journal of Coal Geology*, 78: 135–148.

Kislyakov, Y. M., and Shchetochkin, V.N., 2000. *Hydrogenic ore Formation. Geoinformmark*, Moscow, 238–608 (in Russian).

Li, M., Shao, L.Y., Lu, J., Spiro, B., Wen, H.J., and Li, Y.H., 2014. Sequence stratigraphy and paleogeography of the Middle Jurassic coal measures in the Yuqia coalfield, northern Qaidam Basin, northwestern China. *AAPG Bulletin*, 98: 2531–2550.

Li Shengxiang, Han Xiaozhong, Cai Yuqi, Zheng Enjiu and Wang Baoqun, 2006. Depositional system of the Lower-

Middle Jurassic Shuixigou Group in the western segment of the southern margin of the Yili Basin and its controns on uranium mneralization. *Geology in China*, 33(3): 582–590 (in Chinese with English abstract).

Liu, Y., Jiang, S.H., Bagas, L., Han, N., Chen, C.L., and Kang, H., 2017. Isotopic(C-O-S) geochemistry and Re-Os geochronology of Haobugao Zn-Fe deposit in Inner Mongolia, NE China. *Ore Geology Reviews*, 82: 130–147.

Liu Zhangyue, Peng Suping, Qin Mingkuan, Liu Hongxun, Huang Shaohua, He Zhongbo, Guo Qiang, Xu Qiang and Song Jiye, 2017. Multistage enrichment of the Sawafuqi uranium deposit: new insights into sandstone-hosted uranium deposits in the Intramontane Basins of Tian Shan, China. *Acta Geologica Sinica* (English Edition), 91(6): 2138–2152.

Luo Xiaorong, Sun Ying, Wang Liqun, Xiao Ancheng, Ma Lixie, Zhang Xiaobao, Wang Zhaoming and Song Chengpeng, 2013. Dynamics of hydrocarbon accumulation in the west section of the northern margin of the Qaidam Basin, NW China. *Petroleum Exploration and Development*, 40(2): 159–170 (in Chinese with English abstract).

Lü Baofeng, Zhang Yueqing and Yang Shuyi, 2011. Characteristics of structural system and its implication for formation dynamics in Qaidam Basin. *Geological Review*, 57 (2): 167–173 (in Chinese with English abstract).

Macaulay, C.I, Haszeldine, R.S., and Fallick, A.E., 1993. Distribution, chemistry, isotopic composition and origin of diagenetic carbonates: Magnus sandstone, North Sea. *Journal of sedimentary Petrology*, 63: 33–43.

Maithani, P.B., Taneja, P.C., and Singh, Rajendra, 1995. A sandstone-type uranium deposits at Phlangdiloin, West Khasi Hills, Meghalaya, India. *Journal of Atomic Mineral Science*, 3: 33–60.

Mastalerz, M., and Drobniak, A., 2012. Gallium and germanium in selected Indiana coals. *International Journal of Coal Geology*, 94: 302–313.

Miall, A.D., 1985. Architectural-element analysis: a new method of facies analysis applied to fluvial deposits. *Earth Science Reviews*, 22(4): 261–308.

Miall, A.D., and Jones, B.G., 2003. Fluvial architecture of the Hawkesbury Sandstone (Triassic) near Sydney, Australia. *Journal of Sedimentary Research*, 73(4): 531–545.

Mostafa, F., Harrison, T.M., and Grove, M., 2001. In situ stable isotopic evidence for protracted and complex carbonate cementation in a petroleum reservoir, North Coles Levee, San Joaquin Basin, California, USA. *Journal of Sedimentary Research*, 71(3): 444–458.

Nash, J.T., Granger, H.C., and Adam, S.S., 1981. Geology and concepts of fenesis of important types of uranium deposits. *Economy Geology*, 75: 63–116.

Nxumalo, V., Kramers, J., Mongwaketsi, N., and Przybylowicz, W.J., 2017. Micro-PIXE characterization of uranium occurrence in the coal zones and the mudstones of the Speringbok Flats Basin, South Africa. *Nuclear Instruments and Methods in Physics Research Section B: Beam Interactions with Materials and Atoms*, 404: 114–120.

OECD/NEA-IAEA. 2014. *Uranium Resources, production and Demand, 2013 Red Book.* OECD, Paris, France.

Polito, P.A., Kyser, T.K., and Jackson, M.J., 2006. The role of sandstone diagenesis and aquifer evolution in the Formation of uranium and zinc-lead deposits, Southern McArthur Basin, Northern Territory, Australia. *Economic Geology*, 101(6): 1189–1209.

Qiu Yubo, Yi Haisheng, Zhang Zhanfeng, Wang Guo, Liu Junping, Jiang Hong, Zhang Hujun, Li Yanlong and Hao Yize, 2015. Lithology-lithofacies characteristics and its relationship to uranium deposit of Lower Xishanyao Formation in Kuosijiaer area of Yili Basin. *Acta Sedimentologica Sinica*, 33(4): 687–696 (in Chinese with English abstract).

Ravenhurst, C.E., Reynolds, P.H., Zeneilli, M., Krueger, H.W., and Blenkinsop, J. 1989. Formation of carboniferous Pb-Zn and barite mineralization from basin-derived fluids, Nova Scotia, Canada. *Economic Geology*, 84: 1471–1488.

Ritch, R.A., Holland, H.D., and Petersen, U., 1977. *Hydrothermal Uranium Deposits*. Elsevier Applied Science.

Rong Hui, Jiao Yangquan, Wu Liqun, Ji Dongmin, Li Hongliang, Zhu Qiang, Cao Minqiang, Wang Xiaomei, Li Qingchun and Xie Huili, 2016. Epigenetic alteration and its constraints on uranium mineralization from the Qianjiadian Uranium Deposit, Southern Songliao Basin. *Earth Science*, 41 (1): 153–166 (in Chinese with English abstract).

Sanford, R.F., 1994. A quantitative model of ground-water flow during formation of tabular sandstone type uranium deposits. Economy Geology, 89: 341–360.

Seredin, V.V., 2012, From coal science to metal production and environmental protection: a new story of success. *International Journal of Coal Geology*, 90–91: 1–3.

Seredin, V.V., and Finkelman, R.B., 2008. Metalliferous coals: a review of the main genetic and geochemical types. *International Journal of Coal Geology,* 76: 253–289.

Seredin, V.V., Dai, S.F., Sun, Y.Z., Chekryzhov, and Yu, I., 2013. Coal deposits as promising sources of rare metals for alternative power and energy-efficient technologies. *Applied Geochemistry*, 31: 1–11.

Shao Longyi, Li Meng, Li Yonghong, Zhang Yunpeng, Lu Jing, Zhang Wenlong, Tian Zheng and Wen Huaijun, 2014. Geological characteristics and controlling factors of shale gas in the Jurassic of the northern Qaidam Basin. *Earth Science Frontiers*, 21(4): 311–322 (in Chinese with English abstract).

Shatalov, V.V., Takhanov, A.V., Boldyrev, V.A., and Knyazea, O.I., 2006. Analysis of uranium world resources and ways of their extension. *In: Uranium production and raw materials for the nuclear fuel cycle- Supply and demand, economics, the environment and energy security.* IAEA-CN-128, IAEA, Vienna, 103–110.

Shikazono, N., and Utada, M., 1997. Stable isotope geochemistry and diagenetic mineralization associated with the Tono sandstone-type uranium deposit in Japan. *Mineralium Deposita*, 32: 596–606.

Spirakis, C.S., 1996. The roles of organic matter in the formation of uranium deposits in sedimentary rocks? *Ore Geology Reviews*, 11: 53–69.

Sun, Y.L., Qi, G.X., Lei, X.F., Xu, H., and Wang, Y., 2016. Ectraction of uranium in bottom ash derived from high-germanium coals. *Procedia Environmental Sciences*, 31: 589–597.

Swaine, D.J., 1990. *Trace Elements in Coal*. London: Butterworths.

Tang Liangjie, Jin Zhijun, Zhang Mingli, You Fubao, Zhang Bingshan and Luo Jing, 2000. Tectonic evolution and oil (gas) pool-forming stage in northern Qaidam Basin. *Petroleum Exploration and Development*, 27(2): 36–39 (in Chinese with

English abstract).

Tong Hangshou, 2014. Study on the classification of uranium deposits in China (I). *World Nuclear Geoscience*, 31(1): 1–9 (in Chinese with English abstract).

Turner, C.E., Fishman, N.S., Hatcher, P.G., and Spiker, E.C., 1993. Nature and role of organic matter in sandstone type uranium deposits, Grants uranium region, New Mexico, USA. In: Bitumens in Ore Deposits, Springer Berlin Heidelberg, pp. 239–275.

Wang Dan, 2015. *Oil-gas-coals and sandstone type uranium deposit coexists in the North margin of Qaidam Basin and its geology significance*. Xi'an: Northwest University (Ph. D thesis): 1–-82 (in Chinese).

Wang Dan, Wu Bolin, Cun Xiaoni, Sun Li, Xu Zigao, Zhan Jie and Yuan Kang, 2015. Coexistence of multiple energy minerals in Qaidam Basin and its geological significance. *Journal of Earth Sciences and Environment*, 37(3): 55–67 (in Chinese with English abstract).

Wang Feifei, Liu Chiyang, Niu Haiqing, Deng Yu, Ma Huanhuan and Wang Wenqing, 2017. Global uranium resources in sedimentary basins and the characteristics of oil, gas, coal and uranium coexisting in one basin. *Acta Geologhica Sinica* (English Edition), 91(Z1): 235–236.

Wignall, P.B., 1994. *Black Shales*. Oxford: Clarendon Press, 1–125.

Williams, P.F., and Rust, B.R., 1969. Sedimentology of a braided river. *Journal of Sedimentary Research*, 39: 649–679.

Wu Bolin, Liu Chiyang, Zhang Fuxin, Fang Xiyan and Liu Xiong, 2006. Geochemical characteristics of epigenetic alteration in Dongsheng Sandstone-type Uranium Deposit and its metallogenic signification. *Acta Geologica Sinica*, 80(5): 740–747 (in Chinese with English abstract).

Wu, L.Q., Jiao, Y.Q., Roger, M., and Yang, S.K., 2009. Sedimentological setting of sandstone-type uranium deposits in coal measures on the southwest margin of the Turpan-Hami Basin, China. *Journal of Asian Earth Sciences*, 36(2): 223–237.

Wülser, P.A., Brugger, J., and Foden, J., 2011. The sandstone-hosted Beverley uranium deposit, Lake Frome Basin, South Australia: mineralogy, geochemistry, and a time-constrained model for its genesis. *Economic Geology*, 106(5): 835–867.

Yang Minghui and Liu Chiyang, 2006. Sequence stratigraphic framework and its control on accumulation of various energy resources in the Mesozoic continental basins in Ordos. *Oil & Gas Geology*, 27(4): 563–570 (in Chinese with English abstract).

Yang Renchao, Han Zuozhen and Fan Aiping, 2007. Sedimentary microfacies and sequence stratigraphy of sandstone-type uranium deposit in the Dongsheng area of the Ordos Basin. *Journal of Stratigraphy*, 31(3): 261–266 (in Chinese with English abstract).

Yang Yongtai, Zhang Baomin, Li Wei and Qu Hui, 2000. Study of Jurassic stratigraphic sequence and sedimentary facies in north of Qaidam Basin. *Earth Science Frontiers*, 7(3): 145–151 (in Chinese with English abstract).

Yang Yongtai, Zhang Baomin., Xi Ping, Yu Huilong, Wu Guangda and Liu Dong, 2001. New knowledge about distribution of the Jurassic strata along north margin of Qaidam Basin. *Journal of stratigraphy*, 25(2): 154–158 (in Chinese with English abstract).

Zeng Lianbo, Jin Zhijun, Tang Langjie, Li Jingchang, You Fubao and Zhang Bingshan, 2001. Structural controls of petroleum and gas distribution on northern margin of Qaidam Basin. *Earth Science*, 26(1): 54–58 (in Chinese with English abstract).

Zhai Zhiwei, Zhang Yongshu, Yang Hongmei, Sha Wei, Nian Xiuqing, Hao Xiaomei, Ren Qian and Zhang Jianjie, 2013. Characteristics of effective source rocks in the Jurassic and hydrocarbon accumulation patterns in the areas near the northern margin of the Qaidam Basin. *Natural Gas Industry*, 33(9): 36–42 (in Chinese with English abstract).

Zhang Jindai, Li Youliang and Jian Xiaofei, 2008. Situation and development prospect of uranium resources exploration in China. *Engineering Sciences*, 10(1): 54–60 (in Chinese with English abstract).

Zhang Jindai, Li Ziying, Cai Yongqi, Guo Qingyin, Li Youliang and Han Changqing, 2012. The main advance and achievements in the potential evaluation of uranium resource in China. *Uranium Geology*, 28(6): 321–326 (in Chinese with English abstract).

About the first author

GUO Biao, Male, born in 1985 in Nanyang City, Henan Province, received his doctor's degree from College of Geosciences and Survey Engineering, China University of Mining and Technology in 2015. His major interest focuses on sedimentology and palaeogeography. E-mail: guobiao511@163.com.